

NUMERICAL RANGES OF NON-NORMAL RANDOM MATRICES: ELLIPTIC GINIBRE AND NON-HERMITIAN WISHART ENSEMBLES

SUNG-SOO BYUN AND JOO YOUNG PARK

ABSTRACT. The numerical range of a non-normal matrix plays a central role as a descriptor of non-normal effects beyond spectral information. We study a class of fundamental non-Hermitian random matrix ensembles that interpolate between the Hermitian and non-Hermitian regimes. Our analysis focuses on the elliptic Ginibre ensemble and its chiral counterpart, as well as on non-Hermitian Wishart matrices. For each of these models, we explicitly characterise the geometry of the numerical range in the large-system limit. In particular, we show that for the elliptic Ginibre ensemble and its chiral version, the limiting numerical range is an ellipse, whereas for the non-Hermitian Wishart ensemble it is described by a non-elliptic envelope. Furthermore, we determine the numerical range of products of n independent elliptic Ginibre matrices, which recovers, in the cases $n = 1$ and $n = 2$, the results for the elliptic Ginibre ensemble and the non-Hermitian Wishart ensemble at maximal non-Hermiticity, respectively.

1. INTRODUCTION AND MAIN RESULTS

In random matrix theory, normal matrices are largely governed by their spectral statistics, a fact that allows their behaviour to be understood primarily through eigenvalue distributions. By contrast, non-normal matrices exhibit a range of genuinely new phenomena such as substantial eigenvector overlaps [4, 5, 16, 22, 28, 32], sensitivity to perturbations [13, 33], and the emergence of pseudospectrum [17, 43]. These effects highlight intrinsic limitations of purely spectral descriptions and naturally motivate the study of operator-valued objects that go beyond the spectrum.

Among these objects, the *numerical range* (also known as the *field of values*) [35, 37] plays a central role in capturing non-normal effects beyond the spectrum. For a square matrix $A \in \mathbb{C}^{N \times N}$, it is defined as

$$(1.1) \quad W(A) := \{(Ay, y) : \|y\|_2 = 1\}.$$

While the numerical range coincides with the eigenvalue spectrum for normal matrices, in the non-normal case it is in general a strictly larger convex set that contains the eigenvalue spectrum [39]. As such, it provides a robust descriptor of non-normal behaviour and often reveals geometric or stability properties that remain invisible at the level of the spectrum alone. Moreover, the numerical range serves as an effective tool for analysing convergence rates of iterative schemes for solving linear systems [29, 46].

On the other hand, non-Hermitian random matrix theory has attracted considerable attention in recent years, motivated by a broad range of applications and structural phenomena that go beyond the Hermitian setting; see e.g. [18] and references therein. A fundamental model in this area is the complex Ginibre matrix, an $N \times N$ matrix with i.i.d. complex Gaussian entries of mean zero and variance $1/N$. A classical result for this model is the circular law, which states that the empirical eigenvalue distribution converges to the uniform measure on the centred unit disc as $N \rightarrow \infty$. Despite the long history of the Ginibre ensemble, its numerical range was investigated only relatively recently. It was shown in the seminal work [25] that the numerical range converges to the centred disc of radius $\sqrt{2}$ as $N \rightarrow \infty$. More recently, the sharp convergence rates and fluctuations for the numerical radius of random matrix with general i.i.d. entries were established in [10], building on earlier results on small deviation tail estimates and correlation–decorrelation transitions for Wigner matrices [11, 12].

Beyond the Ginibre matrix whose eigenvalue spectra follow the circular law, there exist several variants of non-Hermitian random matrices, for instance those with correlated entries. In such models, the limiting eigenvalue distribution typically departs from radial symmetry and instead converges to a non-circular measure supported on a domain of nontrivial geometry, often referred to as the *droplet*. While the geometric properties of these spectral limits have been extensively studied (see e.g. [19] and references therein), the corresponding numerical ranges have so far not been systematically investigated.

In this work, we pursue this direction by analysing several well-studied non-Hermitian random matrix ensembles, with particular emphasis on the elliptic Ginibre ensemble and its chiral counterpart, as well as a non-Hermitian Wishart ensemble. These models provide natural non-Hermitian extensions of the classical Gaussian and Laguerre unitary ensembles (GUE and LUE, respectively) [30].

We begin by introducing the random matrix models and their basic statistical properties. In these models, a non-Hermiticity parameter $\tau \in [0, 1]$ plays a central role.

- **Elliptic Ginibre matrix.** The elliptic Ginibre matrix is one of the most extensively studied models interpolating between Hermitian and non-Hermitian random matrices. It is constructed by a linear interpolation between the Hermitian and anti-Hermitian parts of the Ginibre matrix:

$$(1.2) \quad X^e := \frac{\sqrt{1+\tau}}{2}(G + G^*) + \frac{\sqrt{1-\tau}}{2}(G - G^*),$$

where G is the complex Ginibre matrix. In particular, X^e reduces to the Ginibre matrix when $\tau = 0$, and to the GUE when $\tau = 1$. It is well known, under the name of the *elliptic law*, that the eigenvalues of the elliptic Ginibre matrix converge to the uniform distribution on an ellipse

$$(1.3) \quad S^e := \left\{ (x, y) \in \mathbb{R}^2 : \left(\frac{x}{1+\tau} \right)^2 + \left(\frac{y}{1-\tau} \right)^2 \leq 1 \right\}.$$

See Figure 1 (A)–(D). We refer the reader to [18, Section 2.3] for further references on this model.

- **Chiral elliptic Ginibre matrix.** The chiral version of the elliptic Ginibre matrix was introduced in the context of quantum chromodynamics with chemical potential [1, 48, 49]. In this model, one introduces an additional non-negative parameter ν , and considers two $N \times (N + \nu)$ random matrices P and Q with independent complex Gaussian entries of mean zero and variance $1/(2N)$. These matrices serve as building blocks for the correlated matrices

$$(1.4) \quad X_1 := \sqrt{1+\tau}P + \sqrt{1-\tau}Q, \quad X_2 := \sqrt{1+\tau}P - \sqrt{1-\tau}Q.$$

The chiral elliptic Ginibre matrix is then defined as a random Dirac matrix of size $(2N + \nu) \times (2N + \nu)$:

$$(1.5) \quad X^{ce} := \begin{bmatrix} 0 & X_1 \\ X_2^* & 0 \end{bmatrix}.$$

When $\tau = 1$ this model reduces to the standard Hermitian chiral GUE [30, Section 3.1]. In order to describe the macroscopic behaviour of this model, one makes use of the scaling

$$(1.6) \quad \lim_{N \rightarrow \infty} \frac{\nu}{N} = \alpha \in [0, \infty).$$

Then it was shown in [3, Corollary 2] that the random eigenvalues tend to occupy the compact set enclosed by the quartic curve with equation:

$$(1.7) \quad S^{ce} := \left\{ (x, y) \in \mathbb{R}^2 : (x^2 + y^2)^2 + \frac{16\tau^2}{(1-\tau^2)^2} x^2 y^2 - 2\tau(2+\alpha)(x^2 - y^2) \leq (1+\alpha - \tau^2)(1 - (1+\alpha)\tau^2) \right\}.$$

In particular, when $\alpha = 0$, this compact set reduces to the ellipse defined in (1.3). A notable feature of S^{ce} is that for $\alpha > 0$, its topology exhibits a phase transition: if $\tau < 1/\sqrt{1+\alpha}$, the droplet is connected, whereas if $\tau > 1/\sqrt{1+\alpha}$, it consists of two connected components. See Figure 1 (E)–(H).

- **Non-Hermitian Wishart matrix.** The non-Hermitian Wishart matrix, also known as the sample cross-covariance matrix model, was introduced as a framework for analysing time series based on covariance matrices constructed from time-lagged correlation matrices; see e.g. [15, 40]. It is defined as

$$(1.8) \quad X^w := X_1 X_2^*,$$

where X_1 and X_2 are given by (1.4). When $\tau = 0$, the model reduces to the product of two rectangular Ginibre matrices, whereas in the case $\tau = 1$ it reduces to the LUE. It was shown in [3, Theorem 1] that the eigenvalues tend to occupy the shifted ellipse

$$(1.9) \quad S^w := \left\{ (x, y) \in \mathbb{R}^2 : \left(\frac{x - \tau(2+\alpha)}{(1+\tau^2)\sqrt{1+\alpha}} \right)^2 + \left(\frac{y}{(1-\tau^2)\sqrt{1+\alpha}} \right)^2 \leq 1 \right\}.$$

See Figure 2. We refer the reader to [20] for further references on this model.

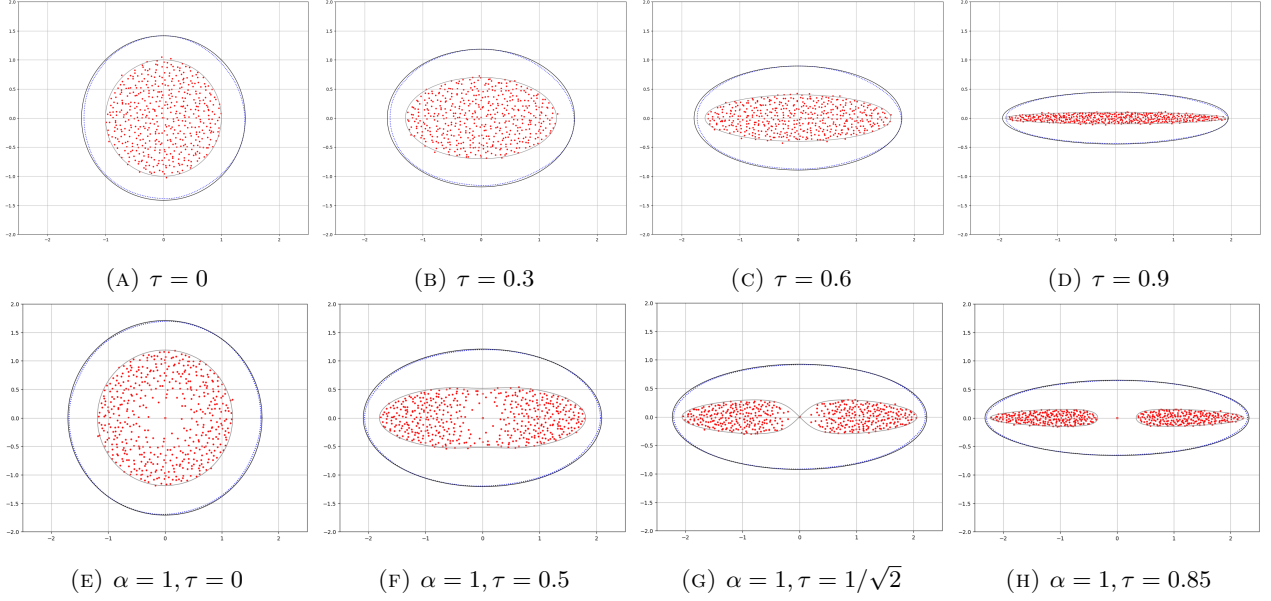


FIGURE 1. The plots display the eigenvalues and numerical ranges of the elliptic Ginibre matrix ((A)–(D)) and the chiral elliptic Ginibre matrix ((E)–(H)). The red dots represent the eigenvalues together with the boundary of the droplet defined in (1.3) and (1.7), respectively. The solid black curves indicate the theoretical numerical ranges given in Theorem 1.1. The blue dotted curves show numerically computed numerical ranges, which are in good agreement with the theoretical results. Here, $N = 500$ for (A)–(D), while $N = 250$ for (E)–(H).

In this work, we determine the limiting numerical range for each of the three models introduced above. We begin by presenting our results for the elliptic Ginibre matrix and its chiral counterpart. For $a, b > 0$, we write

$$(1.10) \quad E_{a,b} := \left\{ (x, y) \in \mathbb{R}^2 : (x/a)^2 + (y/b)^2 \leq 1 \right\}.$$

We also denote by

$$(1.11) \quad d_H(X, Y) := \max \left\{ \sup_{x \in X} d(x, Y), \sup_{y \in Y} d(X, y) \right\}$$

the Hausdorff distance between two subsets X and Y of the complex plane.

Theorem 1.1 (Numerical range of elliptic and chiral elliptic Ginibre matrices). *Let $\tau \in [0, 1]$.*

(i) **(Elliptic Ginibre matrix)** *Let X^e be the elliptic Ginibre matrix of size N . Then we have*

$$(1.12) \quad \lim_{N \rightarrow \infty} d_H(W(X^e), E_{a,b}) = 0,$$

almost surely, where

$$(1.13) \quad a \equiv a(\tau) := \sqrt{2(1+\tau)}, \quad b \equiv b(\tau) := \sqrt{2(1-\tau)}.$$

(ii) **(Chiral elliptic Ginibre matrix)** *Let X^{ce} be the chiral elliptic Ginibre matrix of size $2N + \nu$. Assume that ν scales proportionally to N as specified in (1.6). Then we have*

$$(1.14) \quad \lim_{N \rightarrow \infty} d_H(W(X^{ce}), E_{a,b}) = 0,$$

almost surely, where

$$(1.15) \quad a \equiv a(\tau, \alpha) := \frac{\sqrt{1+\tau}(\sqrt{1+\alpha}+1)}{\sqrt{2}}, \quad b \equiv b(\tau, \alpha) := \frac{\sqrt{1-\tau}(\sqrt{1+\alpha}+1)}{\sqrt{2}}.$$

See Figure 1 for the numerics on Theorem 1.1. Note that, when $\alpha = 0$, the values of a and b in (1.15) coincide with those in (1.13).

Remark 1 (Outer and inner numerical radii). In Theorem 1.1, the major and minor axes a and b are referred to as the outer and inner numerical radii, respectively. For the elliptic Ginibre matrix, the values of a and b in (1.13) were identified in [10, Theorem 1.4], where the sharp error estimate and the corresponding fluctuation behaviour were also established. In contrast to the numerical radius, the statistics of extremal eigenvalues have been extensively studied. We refer to [14, 23, 24, 26, 27, 38, 50] and the references therein for such results concerning various non-Hermitian random matrix ensembles.

Remark 2 (Extension beyond the Gaussian setting). In Theorem 1.1, the models are formulated using matrices with Gaussian entries. However, the argument extends without difficulty to ensembles with more general entries. The essential input in the proof is the almost sure convergence of the largest eigenvalue of the Hermitian part of the matrix. In the case of the elliptic Ginibre ensemble, this Hermitian part belongs to the GUE, for which the convergence of the largest eigenvalue is classical. More generally, the same convergence holds for Wigner matrices under standard moment assumptions (see e.g. [8, 9]). Consequently, Theorem 1.1 remains valid beyond the Gaussian setting, aligning with the universal appearance of the elliptic law [6, 44].

We now present our result for the non-Hermitian Wishart ensemble. Unlike the previous models, the resulting geometry is no longer simply described by an ellipse. To characterise it, we introduce a family of quartic polynomials parametrised by an angular variable. For $\theta \in [0, 2\pi)$, set $c := \cos \theta$ and define

$$(1.16) \quad D_\theta(x) := a_4 x^4 + a_3 x^3 + a_2 x^2 + a_1 x + a_0,$$

where

$$(1.17) \quad \begin{aligned} a_4 &= 16(1 - \tau^2 + c^2 \tau^2), & a_3 &= -32 c \tau (\alpha + 2)(1 - \tau^2 + c^2 \tau^2), \\ a_2 &= 16\alpha^2 c^4 \tau^4 + 4(\alpha^2 - 8\alpha - 11)(1 - \tau^2)^2 + 8c^2 \tau^2 (2\alpha^2 - 5\alpha - 6)(1 - \tau^2), \\ a_1 &= 4 c \tau (1 - \tau^2) (2\alpha^2 c^2 \tau^2 - (1 - \tau^2)(2\alpha^3 + 5\alpha^2 + 8\alpha + 3)), \\ a_0 &= (2\alpha + 1)^2 (1 - \tau^2)^2 (\alpha^2 c^2 \tau^2 - (2\alpha + 1)(1 - \tau^2)). \end{aligned}$$

The equation $D_\theta(x) = 0$ has exactly two distinct real roots; see Lemma 3.1 below. We denote by $\lambda(\theta)$ the larger of these two roots. We write $H_\theta := e^{-i\theta} \{z \in \mathbb{C} : \operatorname{Re} z \leq \lambda(\theta)\}$, and define

$$(1.18) \quad \tilde{E}(\tau, \alpha) := \bigcap_{0 \leq \theta \leq 2\pi} H_\theta.$$

See Figure 9 for an illustration of this domain.

Theorem 1.2 (Numerical range of non-Hermitian Wishart matrix). *Let $\tau \in [0, 1]$. Let X^w be the non-Hermitian Wishart matrix of size N . Assume that ν scales proportionally to N as specified in (1.6). Then we have*

$$(1.19) \quad \lim_{N \rightarrow \infty} d_H(W(X^w), \tilde{E}(\tau, \alpha)) = 0,$$

almost surely, where $\tilde{E}(\tau, \alpha)$ is given by (1.18).

See Figures 2 and 9 for the numerics on Theorem 1.2. The proof of Theorem 1.2 proceeds via a structural reformulation of the Hermitian part $\operatorname{Re}(e^{i\theta} X^w)$. Exploiting a spectral decomposition together with the Gaussian invariance of the ensemble, we reduce the problem to two Wishart-type components. This approach contrasts with the elliptic Ginibre case in Remark 2, as it depends essentially on the Gaussian nature of the entries.

Remark 3 (Maximally non-Hermitian case; products of two rectangular Ginibre matrices). In the special case $\tau = 0$, the polynomial (1.16) simplifies to

$$(1.20) \quad D_\theta(x)|_{\tau=0} = 16x^4 + 4(\alpha^2 - 8\alpha - 11)x^2 - (2\alpha + 1)^3.$$

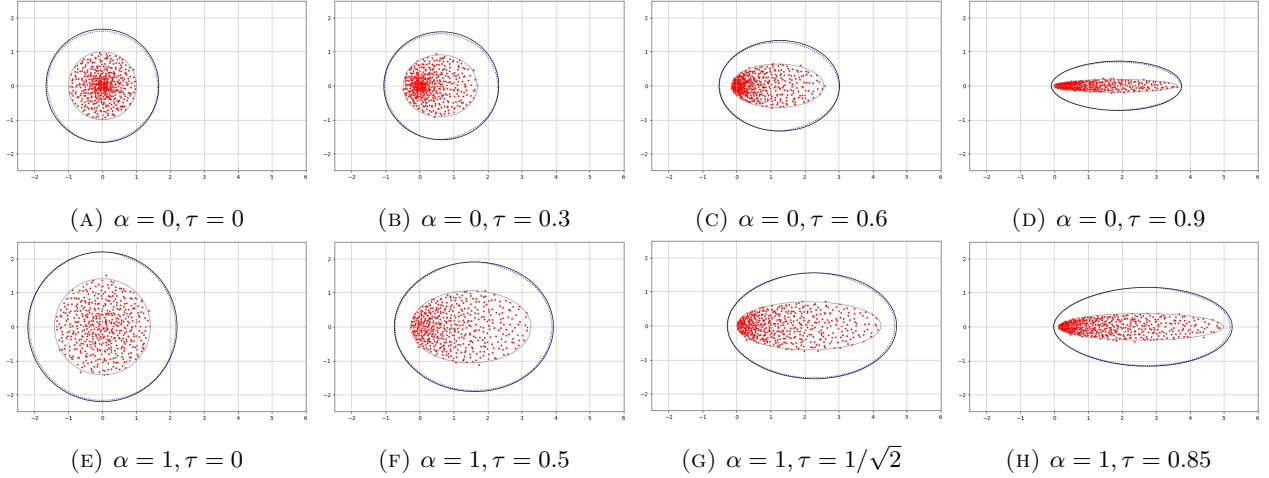


FIGURE 2. The same figure as in Figure 1 for the non-Hermitian Wishart ensemble. The solid black curve indicates the theoretical numerical range given in Theorem 1.2. Here, $N = 500$.

In this case, the expression is independent of the angular parameter θ . The real roots of $D_\theta(x)|_{\tau=0}$ are given by $\pm B$, where

$$(1.21) \quad B := \sqrt{\frac{-\alpha^2 + 8\alpha + 11 + (\alpha + 5)\sqrt{\alpha^2 + 6\alpha + 5}}{8}}.$$

Consequently, it follows that

$$(1.22) \quad \tilde{E}(0, \alpha) = \mathbb{D}(B).$$

where $\mathbb{D}(r) = \{z \in \mathbb{C} : |z| \leq r\}$.

Remark 4 (Hermitian limits). In our models, taking the limit $\tau \rightarrow 1$ yields a Hermitian matrix ensemble. In this regime, the numerical range is expected to coincide with the convex hull of the eigenvalue spectrum, a phenomenon that can be directly verified from our explicit results.

For the elliptic Ginibre ensemble, the spectral droplet defined in (1.3) collapses to the interval $[-2, 2]$ as $\tau \rightarrow 1$. This interval is precisely the support of the semicircle law of the GUE. Consistently, from (1.13) we have $a(1) = 2$, in agreement with this limiting behaviour.

For the chiral elliptic Ginibre ensemble, the spectral droplet defined in (1.7) converges, as $\tau \rightarrow 1$, to the union of two disjoint intervals

$$(1.23) \quad [-\sqrt{\lambda_+}, \sqrt{\lambda_-}] \cup [\sqrt{\lambda_-}, \sqrt{\lambda_+}], \quad \lambda_\pm := (\sqrt{\alpha + 1} \pm 1)^2.$$

This set coincides with the support of the limiting spectral distribution of the chiral GUE. On the other hand, it follows from (1.15) that, in the same limit, the numerical range becomes the single interval $[-\sqrt{\lambda_+}, \sqrt{\lambda_+}]$, which is precisely the convex hull of the above two-cut spectral support.

For the non-Hermitian Wishart ensemble, as $\tau \rightarrow 1$, the spectral droplet collapses to the interval $[\lambda_-, \lambda_+]$, which coincides with the support of the Marchenko–Pastur law of the LUE. To analyse the Hermitian limit of the numerical range, we observe that the polynomial in (1.16) simplifies to $D(x)|_{\tau=1} = 16x^2(\alpha - x)^2 - 64x^3$. Its real roots are given by $x = 0$ and $x = \lambda_\pm$. Consequently, the numerical range in the Hermitian limit is the interval $[\lambda_-, \lambda_+]$, in agreement with the spectral support.

Remark 5 (Geometry of numerical range of non-Hermitian Wishart matrix). In contrast to the elliptic and chiral elliptic Ginibre matrices considered in Theorem 1.1 whose numerical ranges are given by ellipses, the numerical range of the non-Hermitian Wishart matrix in Theorem 1.2 exhibits a markedly different behaviour. Although it is a convex subset of the complex plane and bears a superficial resemblance to an ellipse, it is in fact not an ellipse; see Appendix A for more discussions.

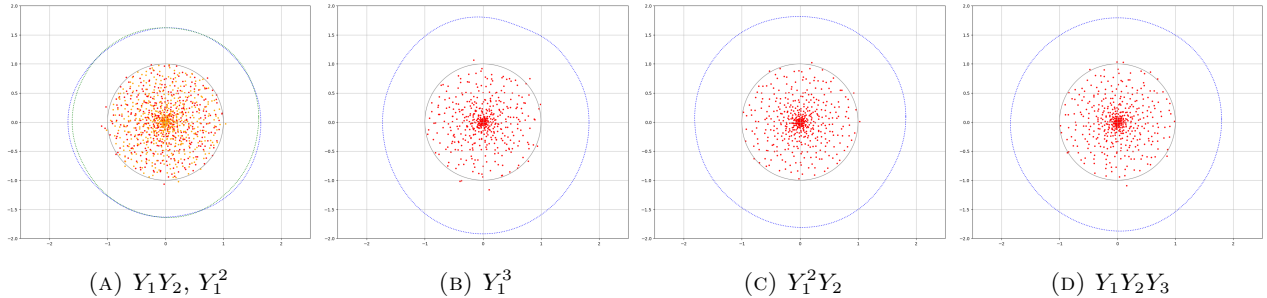


FIGURE 3. The plots display the eigenvalues and simulated numerical ranges for products and powers of Ginibre matrices Y_k , where the matrices are normalised so that the associated droplet is the unit disc. In (A), we compare the product of two independent Ginibre matrices with the square of a single Ginibre matrix; in both cases, the numerical radius coincides with the value in (1.24). Figures (B)–(D) show numerical ranges for various combinations of products and powers involving three Ginibre matrices. In all cases, the limiting numerical radius appears to be identical. Here, $N = 500$.

Remark 6 (Numerical ranges of products and powers of complex Ginibre matrices). As already noted in Remark 3, the non-Hermitian Wishart matrix is closely related to products of Ginibre matrices; see [18, Section 2.7]. In particular, when $\nu = 0$, the non-Hermitian Wishart matrix coincides with the product of two independent square Ginibre matrices. In this case, specialising (1.21) to $\alpha = 0$, the numerical range is given by a centred disc of radius

$$(1.24) \quad \sqrt{\frac{11 + 5\sqrt{5}}{8}} \asymp 1.665.$$

It is instructive to compare this situation with the case of powers of a Ginibre matrix. While the special case of the non-Hermitian Wishart matrix corresponds to a product Y_1Y_2 of two independent Ginibre matrices, it is fundamentally different from a power of a single Ginibre matrix, such as Y_1^2 . Nevertheless, their limiting global eigenvalue distributions coincide [2, 41]. Numerical simulations presented in Figure 3 (A) suggest that their numerical ranges also coincide in the large- N limit. This phenomenon can indeed be established by adapting the same strategy used in the proof of Theorem 1.2. We further observe that this agreement persists more generally: the numerical ranges of products and powers of Ginibre matrices coincide asymptotically, provided that the total number of Ginibre factors—counted with multiplicity—is the same; cf. Proposition 4.3. See Figure 3 (B)–(D) for the case of three Ginibre factors.

We also briefly comment on the value of the numerical radius in (1.24). In general, several inequalities are known for the numerical radius of a matrix. A classical upper bound, which follows from the submultiplicativity of the numerical radius, states that for any square matrix X , the numerical radius $r(X)$ satisfies

$$(1.25) \quad r(X^2) \leq r(X)^2.$$

Since the value in (1.24) is strictly smaller than 2 (recalling that the numerical radius of the Ginibre matrix is $\sqrt{2}$ due to [25]), the bound (1.25) is not sharp for powers of Ginibre matrices.

Extending the previous remark, we now consider the product model of elliptic Ginibre matrices. Let $n \geq 2$ and let $X_1^e, X_2^e, \dots, X_n^e$ be $N \times N$ i.i.d. elliptic Ginibre matrices. We define the product ensemble

$$(1.26) \quad \mathbf{X}_n^e := X_1^e X_2^e \dots X_n^e.$$

A remarkable fact shown in [47] is that for $n \geq 2$, the limiting eigenvalue distribution of the product model (1.26) does not depend on the non-Hermiticity parameter τ . In particular, the limiting spectrum is supported on the unit disc, with a non-uniform density.

In the following result, we determine the numerical range of this product model. This demonstrates that the above τ -independence phenomenon also persists at the level of the numerical range.

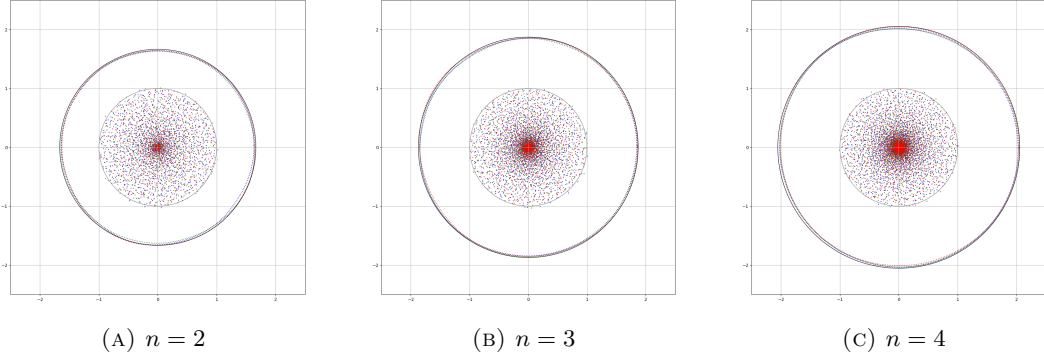


FIGURE 4. The plots display the eigenvalues (dots) and the numerical range (dotted curve) of \mathbf{X}_n^e for $n = 2, 3, 4$ with $N = 500n$, together with the circle of radius R_n defined in (1.28). In each plot, we simultaneously present the cases $\tau = 0, 0.5, 1$, and observe that, for all these values of τ , the numerical ranges asymptotically coincide with the analytic prediction.

Theorem 1.3 (Numerical range of products of eGinUEs). *Let $\tau \in [0, 1]$ and $n \geq 2$. Let \mathbf{X}_n^e be given by (1.26). Then we have*

$$(1.27) \quad \lim_{N \rightarrow \infty} d_H(W(\mathbf{X}_n^e), \mathbb{D}(R_n)) = 0,$$

almost surely, where

$$(1.28) \quad R_n := \frac{\sqrt{n}}{2^{n+\frac{3}{2}}} \left(1 + \sqrt{1 + \frac{8}{n}}\right)^{\frac{3}{2}} \left(3 + \sqrt{1 + \frac{8}{n}}\right)^{\frac{n-1}{2}}.$$

See Figure 4 for a numerical verification of Theorem 1.3.

Note that the first few values of R_n are given by

$$(1.29) \quad R_2 = \sqrt{\frac{11 + 5\sqrt{5}}{8}} \approx 1.665, \quad R_3 = \frac{\sqrt{63 + 11\sqrt{33}}}{6} \approx 1.872, \quad R_4 = \frac{\sqrt{135 + 78\sqrt{3}}}{8} \approx 2.054.$$

Notice that R_2 agrees with the value in (1.24). It is easy to see that R_n is increasing in n , which is consistent with the intuition that the non-normality of products of random matrices increases as the number of factors grows. On the other hand, a straightforward computation shows that as $n \rightarrow \infty$,

$$(1.30) \quad R_n = \frac{\sqrt{en}}{2} + O\left(\frac{1}{\sqrt{n}}\right).$$

In Theorem 1.3, we focus on the product model (1.26) formed from independent eGinUE matrices. However, in the GinUE case when $\tau = 0$, one may also allow the matrices to appear with multiplicity, and the result continues to hold; see Proposition 4.3.

Organisation of the paper. The remainder of this paper is organised as follows. In Section 2, we collect the preliminary material and introduce key lemmas required for the proofs. Section 3 is devoted to the proofs of Theorems 1.1 and 1.2, while Section 4 contains the proof of Theorem 1.3. Finally, in Appendix A, we discuss Remark 5 in more detail with numerical simulations.

Acknowledgements. Sung-Soo Byun was supported by the National Research Foundation of Korea grants (RS-2023-00301976, RS-2025-00516909). We thank Zhigang Bao and Giorgio Cipolloni for helpful comments during the preparation of the paper.

2. PRELIMINARIES

In this section, we collect several basic properties of numerical ranges and present preliminary material needed for the proofs of our main results.

A remarkable property of the numerical range of a non-Hermitian matrix is that it admits an explicit characterisation in terms of its (rotated) Hermitian part. Specifically, let A be an $N \times N$ matrix and $\theta \in [0, 2\pi)$, and denote by $\lambda_{\max}(\theta, N)$ the largest eigenvalue of $\operatorname{Re}(e^{i\theta} A)$. The numerical range $W(A)$ can then be characterised as the intersection of a family of half-planes

$$(2.1) \quad W(A) = \bigcap_{0 \leq \theta \leq 2\pi} H_{\theta, N}, \quad H_{\theta, N} := e^{-i\theta} \{z \in \mathbb{C} : \operatorname{Re}(z) \leq \lambda_{\max}(\theta, N)\}.$$

This property will play a key role in our analysis. Indeed, it was already used in a crucial way in [25, Theorem 4.1], where the following result was established. Let $R > 0$, and let $\{X_N\}_{N \geq 1}$ be a sequence of complex random $N \times N$ matrices such that, for every $\theta \in \mathbb{R}$,

$$(2.2) \quad \lim_{N \rightarrow \infty} \|\operatorname{Re}(e^{i\theta} X_N)\| = R,$$

almost surely. Then

$$(2.3) \quad \lim_{N \rightarrow \infty} d_H(W(X_N), \mathbb{D}(R)) = 0,$$

almost surely. We next introduce a slight extension of this result to the situation in which the limit (2.2) depends on the angular parameter θ . This extension will be used in Theorem 1.1.

Proposition 2.1 (Elliptic numerical range). *Let $a \geq b > 0$, and let $\{X_N\}_{N \geq 1}$ be a sequence of complex random $N \times N$ matrices such that, for every $\theta \in \mathbb{R}$,*

$$(2.4) \quad \lim_{N \rightarrow \infty} \|\operatorname{Re}(e^{i\theta} X_N)\| = \sqrt{a^2 \cos^2 \theta + b^2 \sin^2 \theta},$$

almost surely. Then we have

$$(2.5) \quad \lim_{N \rightarrow \infty} d_H(W(X_N), E_{a,b}) = 0,$$

almost surely. Here, $E_{a,b}$ is an ellipse given by (1.10).

To establish such a lemma, it is convenient to formulate a general statement that allows one to apply the Toeplitz–Hausdorff theorem under uniform convergence. We present this statement below.

Lemma 2.2. *Let $\{X_N\}_{N \geq 1}$ be a sequence of complex random $N \times N$ matrices, and denote by $\lambda_{\max}(\theta, N)$ the largest eigenvalue of $\operatorname{Re}(e^{i\theta} X_N)$. Suppose that, for every $\theta \in [0, 2\pi]$,*

$$(2.6) \quad \lim_{N \rightarrow \infty} \lambda_{\max}(\theta, N) = \lambda(\theta),$$

almost surely. For $\theta \in [0, 2\pi]$, define

$$(2.7) \quad E := \bigcap_{0 \leq \theta \leq 2\pi} H_{\theta}, \quad H_{\theta} := e^{-i\theta} \{z \in \mathbb{C} : \operatorname{Re}(z) \leq \lambda(\theta)\}.$$

Assume furthermore that $\lambda(0) + \lambda(-\frac{\pi}{2}) < \infty$. Then we have

$$(2.8) \quad \lim_{N \rightarrow \infty} d_H(W(X_N), E) = 0,$$

almost surely.

Proof. This statement provides a slight extension of [25, Theorem 4.1]. The proof follows the same general strategy, with only minor modifications to the original argument. Note that

$$\begin{aligned} \limsup_{N \rightarrow \infty} \|X_N\| &\leq \limsup_{N \rightarrow \infty} \|\operatorname{Re}(X_N)\| + \limsup_{N \rightarrow \infty} \|\operatorname{Im}(X_N)\| \\ &= \limsup_{N \rightarrow \infty} \|\operatorname{Re}(X_N)\| + \limsup_{N \rightarrow \infty} \|\operatorname{Re}(e^{-i\frac{\pi}{2}} X_N)\| = \lambda(0) + \lambda(-\frac{\pi}{2}) < \infty. \end{aligned}$$

Write $C := \sup_{N \rightarrow \infty} \|X_N\| < \infty$. Note that for all N and $\theta, \phi \in [0, 2\pi]$, we have

$$|\lambda_{\max}(\theta, N) - \lambda_{\max}(\phi, N)| \leq \|\operatorname{Re}(e^{i\theta} X_N) - \operatorname{Re}(e^{i\phi} X_N)\| \leq |e^{i\theta} - e^{i\phi}| \cdot \|X_N\| \leq C|\theta - \phi|.$$

Therefore by taking the limit $N \rightarrow \infty$, we have $|\lambda(\theta) - \lambda(\phi)| \leq C|\theta - \phi|$.

Fix $\varepsilon > 0$. Choose $\delta > 0$ so that $C\delta < \frac{\varepsilon}{3}$, and let $\mathcal{N} = \{\theta_1, \dots, \theta_m\} \subset [0, 2\pi]$ be a finite δ -net of $[0, 2\pi]$, i.e. for every $\theta \in [0, 2\pi]$ there exists $\theta_j \in \mathcal{N}$ such that $|\theta - \theta_j| \leq \delta$. By the pointwise convergence assumption, there exists $N_0 \in \mathbb{N}$ such that for all $N \geq N_0$ and all $j \in \{1, \dots, m\}$, $|\lambda_{\max}(\theta_j, N) - \lambda(\theta_j)| < \frac{\varepsilon}{3}$.

Fix $N \geq N_0$ and an arbitrary $\theta \in [0, 2\pi]$, and choose $\theta_j \in \mathcal{N}$ with $|\theta - \theta_j| \leq \delta$. Using the Lipschitz continuity of $\lambda_{\max}(\cdot, N)$ and λ , we obtain

$$|\lambda_{\max}(\theta, N) - \lambda(\theta)| \leq |\lambda_{\max}(\theta, N) - \lambda_{\max}(\theta_j, N)| + |\lambda_{\max}(\theta_j, N) - \lambda(\theta_j)| + |\lambda(\theta_j) - \lambda(\theta)| < \varepsilon.$$

Since θ was arbitrary, this proves the uniform convergence

$$(2.9) \quad \sup_{\theta \in [0, 2\pi]} |\lambda_{\max}(\theta, N) - \lambda(\theta)| \rightarrow 0, \quad \text{as } N \rightarrow \infty.$$

Define $h_N(\theta) := \lambda_{\max}(\theta, N)$. Then $\|h_N - \lambda\|_\infty \rightarrow 0$ as $N \rightarrow \infty$. Let $z \in W(X_N)$. Note that for any $\theta \in [0, 2\pi]$,

$$\operatorname{Re}(e^{i\theta} z) \leq h_N(\theta) \leq \lambda(\theta) + \|h_N - \lambda\|_\infty < \lambda(\theta) + \varepsilon$$

for all sufficiently large N . Then by (2.1), $W(X_N)$ is contained in the ε -neighbourhood of E . Conversely, if $z \in E$, then for any $\theta \in [0, 2\pi]$,

$$\operatorname{Re}(e^{i\theta} z) \leq \lambda(\theta) \leq h_N(\theta) + \|h_N - \lambda\|_\infty < h_N(\theta) + \varepsilon.$$

Therefore E is contained in the ε -neighbourhood of $W(X_N)$ for sufficiently large N . This completes the proof. \square

Building on Lemma 2.2, we show Proposition 2.1.

Proof of Proposition 2.1. Note that by (2.4), we have $\lambda(0) = a$ and $\lambda(-\frac{\pi}{2}) = b$. Let l_θ denote the line through the origin with argument $\theta \in [0, 2\pi)$. Among the two lines perpendicular to l_θ and tangent to the ellipse $E_{a,b}$, let \tilde{l}_θ be the one lying in the direction of l_θ . Denote by P_θ the intersection point of l_θ and \tilde{l}_θ . A direct computation shows that the distance from the origin to P_θ is given by

$$(2.10) \quad |P_\theta| = \sqrt{a^2 \cos^2 \theta + b^2 \sin^2 \theta},$$

which coincides with (2.4). Therefore, by Lemma 2.2, the desired result follows. \square

We end this section by recalling a few basic notions from free probability theory that will be used in the proof of Theorem 1.2; see e.g. [7, 36, 42, 45] for further background.

Let (\mathcal{A}, ϕ) be a non-commutative probability space, where \mathcal{A} is a unital $*$ -algebra and ϕ is a tracial state. Two self-adjoint elements $a_1, a_2 \in \mathcal{A}$ are said to be *free* if all their mixed centered moments vanish. If a_i has distribution μ_i ($i = 1, 2$), the distribution of $a_1 + a_2$ depends only on μ_1 and μ_2 and is called the *free additive convolution* of μ_1 and μ_2 , denoted by $\mu_1 \boxplus \mu_2$.

Free additive convolution naturally arises as the large- N limit of sums of independent random matrices. More precisely, if A_N and B_N are independent Hermitian random matrices whose empirical spectral measures converge almost surely to compactly supported probability measures μ and ν , respectively, and if U_N is an independent Haar unitary matrix, then A_N and $U_N B_N U_N^*$ are asymptotically free almost surely. Consequently, the empirical spectral measure of $A_N + U_N B_N U_N^*$ converges almost surely to $\mu \boxplus \nu$; see e.g. [36, Proposition 4.3.9].

In order to characterise $\mu \boxplus \nu$, it is convenient to work with analytic transforms. For a compactly supported probability measure μ on \mathbb{R} , its *Cauchy transform* is defined by

$$(2.11) \quad G_\mu(z) = \int_{\mathbb{R}} \frac{1}{z - x} d\mu(x), \quad z \in \mathbb{C} \setminus \mathbb{R}.$$

The measure μ can be recovered from G_μ via the Stieltjes inversion formula. The *R-transform* of μ can be defined implicitly through the functional relation

$$(2.12) \quad G_\mu \left(R_\mu(z) + \frac{1}{z} \right) = z.$$

The central advantage of the *R-transform* is that it linearises free additive convolution: if μ and ν are compactly supported probability measures on \mathbb{R} , then

$$(2.13) \quad R_{\mu \boxplus \nu}(z) = R_\mu(z) + R_\nu(z).$$

3. PROOFS OF THEOREMS 1.3 AND 1.2

In this section, we present the proofs of the main results.

For the reader's convenience, we first recall a well-known result on the almost sure convergence of the extremal eigenvalues of a Wigner matrix; see e.g. [7, Theorem 5.2]. Suppose that the diagonal elements of the Wigner matrix $W_n = (x_{ij})$ are i.i.d. real random variables, the elements above the diagonal are i.i.d. complex random variables, and all these variables are independent. Then, the largest eigenvalue of W_n tends to c_1 and the smallest eigenvalue tends to c_2 almost surely if and only if $\mathbb{E}(x_{11}^2) < \infty$, $\mathbb{E}(x_{12}) = 0$, $\mathbb{E}(|x_{12}|^2) = \sigma^2/n < \infty$, and $c_1 = 2\sigma$, $c_2 = -2\sigma$. The corresponding result for the sample covariance matrix can be found in [7, Theorem 5.10]; see also [8, 9].

3.1. Proof of Theorem 1.1. We first show the result for the elliptic Ginibre ensemble. By the definition of X^e in (1.2), we have

$$(3.1) \quad \operatorname{Re}(e^{i\theta} X^e) = \frac{\sqrt{1+\tau} \cos(\theta) + i\sqrt{1-\tau} \sin(\theta)}{2} G + \frac{\sqrt{1+\tau} \cos(\theta) - i\sqrt{1-\tau} \sin(\theta)}{2} G^*.$$

Observe that this corresponds to a suitably rescaled GUE matrix (or, more generally, a Wigner matrix). Let x_{ij} and g_{ij} denote the (i, j) -th entries of $\operatorname{Re}(e^{i\theta} X^e)$ and G , respectively. A direct computation yields

$$(3.2) \quad x_{11} = \sqrt{1+\tau} \cos(\theta) \operatorname{Re}(g_{11}) - \sqrt{1-\tau} \sin(\theta) \operatorname{Im}(g_{11}),$$

$$(3.3) \quad x_{12} = \frac{\sqrt{1+\tau} \cos(\theta) + i\sqrt{1-\tau} \sin(\theta)}{2} g_{12} + \frac{\sqrt{1+\tau} \cos(\theta) - i\sqrt{1-\tau} \sin(\theta)}{2} \overline{g_{21}}.$$

Consequently, we have

$$(3.4) \quad \mathbb{E}[x_{11}^2] = \frac{(1+\tau) \cos^2(\theta) + (1-\tau) \sin^2(\theta)}{2N},$$

$$(3.5) \quad \mathbb{E}[|x_{12}|^2] = \frac{(1+\tau) \cos^2(\theta) + (1-\tau) \sin^2(\theta)}{2N},$$

and $\mathbb{E}[x_{12}] = 0$. Applying the general convergence result for the extremal eigenvalues of Wigner matrices mentioned above, we obtain

$$(3.6) \quad \lim_{N \rightarrow \infty} \|\operatorname{Re}(e^{i\theta} X^e)\| = \sqrt{2(1+\tau) \cos^2 \theta + 2(1-\tau) \sin^2 \theta}.$$

Then Theorem 1.1 (i) now follows from Proposition 2.1.

We next prove the result for the chiral elliptic Ginibre ensemble. By the definition of X^{ce} in (1.5), we have

$$(3.7) \quad \operatorname{Re}(e^{i\theta} X^{ce}) = \begin{bmatrix} 0 & \sqrt{1+\tau} \cos(\theta)P + i\sqrt{1-\tau} \sin(\theta)Q \\ \sqrt{1+\tau} \cos(\theta)P^* - i\sqrt{1-\tau} \sin(\theta)Q^* & 0 \end{bmatrix}.$$

Since P and Q are independent rectangular Ginibre matrices with Gaussian entries, we have

$$(3.8) \quad \sqrt{1+\tau} \cos(\theta)P + i\sqrt{1-\tau} \sin(\theta)Q \stackrel{d}{=} \sqrt{(1+\tau) \cos^2(\theta) + (1-\tau) \sin^2(\theta)} P.$$

Consequently, it follows that

$$(3.9) \quad \operatorname{Re}(e^{i\theta} X^{ce}) \stackrel{d}{=} \sqrt{(1+\tau) \cos^2(\theta) + (1-\tau) \sin^2(\theta)} \begin{bmatrix} 0 & P \\ P^* & 0 \end{bmatrix}.$$

Note here that the nonzero eigenvalues of the block matrix are given by $\pm \sqrt{\lambda_j}$, where $\{\lambda_j\}$ are the eigenvalues of PP^* . Hence, its spectral norm is equal to $\|P\|$. By the almost sure convergence of the largest eigenvalue of a Wishart matrix to the right edge of the Marchenko–Pastur law, we obtain

$$(3.10) \quad \lim_{N \rightarrow \infty} \|\operatorname{Re}(e^{i\theta} X^{ce})\| = \frac{\sqrt{1+\alpha} + 1}{\sqrt{2}} \sqrt{(1+\tau) \cos^2(\theta) + (1-\tau) \sin^2(\theta)}.$$

Then by Proposition 2.1, we obtain Theorem 1.1 (ii). \square

Remark 7 (Alternative derivation for the elliptic Ginibre matrix). While our proof provides a systematic framework for deriving the numerical range—particularly in the case of an elliptic domain—there is, for the elliptic Ginibre ensemble, a simpler argument available. Indeed, the numerical range may be recovered directly from the corresponding result for the Ginibre ensemble by exploiting the structural relation between the two models.

More precisely, by the definition (1.2), for any $y \in \mathbb{C}^N$ with $\|y\|_2 = 1$, we have

$$y^* X^e y = \frac{\sqrt{1+\tau} + \sqrt{1-\tau}}{2} z + \frac{\sqrt{1+\tau} - \sqrt{1-\tau}}{2} z^*,$$

where we have set $z := y^* G y$. Since z belongs to the numerical range of G , the claim follows from the known description of this set. More specifically, as $N \rightarrow \infty$, it follows from [25] that the numerical range of G converges to the disc $\mathbb{D}(\sqrt{2})$. Hence we may write

$$z = r(\cos \theta + i \sin \theta), \quad 0 \leq r \leq \sqrt{2}, \quad \theta \in \mathbb{R}.$$

Substituting into the above expression yields

$$y^* X^e y = r\sqrt{1+\tau} \cos \theta + i r\sqrt{1-\tau} \sin \theta,$$

which parametrises precisely the ellipse stated in Theorem 1.1 (i).

3.2. Proof of Theorem 1.2. In this subsection, we prove Theorem 1.2. Recall that the quartic polynomial D_θ is defined in (1.16). In Theorem 1.2, the boundary of the numerical range is characterised in terms of the larger of the two real roots of D_θ . We begin by showing that D_θ indeed has exactly two real roots.

Lemma 3.1. *For every $\alpha \geq 0$, $0 < \tau < 1$, and fixed θ , the equation $D_\theta(x) = 0$ has exactly two distinct real roots.*

Proof. Note that by (1.16), the leading coefficient of $D_\theta(x)$ is $16(1 - \tau^2 \sin^2 \theta) > 0$, and a direct computation shows that $D_\theta(\tau \cos \theta \alpha) < 0$. It follows that the equation $D_\theta(x) = 0$ has at least two real roots.

Suppose, for contradiction, that there exist parameters $\alpha' \geq 0$ and $0 < \tau' < 1$ such that $D_\theta(x) = 0$ has more than two real roots. By continuity of the roots with respect to the coefficients of the polynomial, there must then exist parameters (α, τ) for which $D_\theta(x) = 0$ has four real roots, with at least one of them being a double root. We now fix such a pair (α, τ) and show that this leads to a contradiction.

For this, we first recall the definition of the resultant of two polynomials. Let

$$P(x) = a_m x^m + \cdots + a_0, \quad Q(x) = b_n x^n + \cdots + b_0$$

be polynomials of degrees m and n , respectively. The resultant of P and Q is defined as

$$(3.11) \quad \text{Res}(P, Q) := \det S(P, Q),$$

where the Sylvester matrix $S(P, Q)$ is the $(m+n) \times (m+n)$ matrix defined by

$$S(P, Q) = \begin{pmatrix} a_m & a_{m-1} & \cdots & a_0 & 0 & \cdots & 0 \\ 0 & a_m & a_{m-1} & \cdots & a_0 & \ddots & \vdots \\ \vdots & \ddots & \ddots & & & \ddots & 0 \\ 0 & \cdots & 0 & a_m & a_{m-1} & \cdots & a_0 \\ b_n & b_{n-1} & \cdots & b_0 & 0 & \cdots & 0 \\ 0 & b_n & b_{n-1} & \cdots & b_0 & \ddots & \vdots \\ \vdots & \ddots & \ddots & & & \ddots & 0 \\ 0 & \cdots & 0 & b_n & b_{n-1} & \cdots & b_0 \end{pmatrix}.$$

Here, the first n rows consist of shifted copies of the coefficient vector (a_m, \dots, a_0) and the last m rows consist of shifted copies of (b_n, \dots, b_0) . It satisfies the fundamental property that $\text{Res}(P, Q) = 0$ if and only if P and Q have a common root. In particular, a polynomial P has a multiple root if and only if $\text{Res}(P, P') = 0$.

Since $D_\theta(x) = 0$ is assumed to have a real root of multiplicity two, the resultant of $D_\theta(x)$ and its derivative $D'_\theta(x)$ must vanish. A direct computation yields

$$(3.12) \quad \text{Res}(D_\theta, D'_\theta) = -2^{20}(\alpha + 1)^2(1 - \tau)^2(1 + \tau)^2(1 - \tau^2 \sin^2(\theta))F(\alpha, \tau, \sin^2(\theta))^3$$

where $F(\alpha, \tau, u)$ is an explicit polynomial obtained by straightforward computation:

$$(3.13) \quad \begin{aligned} F(\alpha, \tau, u) = & -16\alpha^3\tau^6u^3 + 24\alpha^2\tau^4(\alpha\tau^2 + \alpha + \tau^2 - 1)u^2 \\ & - 3\tau^2\left(4\alpha^3(\tau^2 + 1)^2 + \alpha^2(\tau^2 - 1)(17\tau^2 - 1) + (22\alpha + 9)(\tau^2 - 1)^2\right)u \\ & + 2(\alpha + 1)^3\tau^6 + 3(\alpha + 1)^2(2\alpha + 7)\tau^4 + 6(\alpha + 1)(\alpha^2 - 11\alpha - 8)\tau^2 + (2\alpha + 1)(\alpha + 5)^2. \end{aligned}$$

Moreover, one can observe that $\partial F/\partial u$ is a quadratic polynomial in u , whose discriminant is given by

$$(3.14) \quad \text{Disc}\left(\frac{\partial F}{\partial u}\right) = -5184\alpha^3\tau^8(\alpha + 1)^2(1 - \tau)^2(1 + \tau)^2 < 0.$$

This shows that $F(\alpha, \tau, u)$ is strictly decreasing function in u . Since $\sin^2\theta \in [0, 1]$, it suffices to consider $0 \leq u \leq 1$. Evaluating at $u = 1$, we obtain

$$(3.15) \quad F(\alpha, \tau, 1) = (\alpha + 5)^2(2\alpha + 1)(1 - \tau)^3(1 + \tau)^3 > 0.$$

By monotonicity, it follows that $F(\alpha, \tau, u) > 0$ for all $0 \leq u \leq 1$. Consequently, $\text{Res}(D_\theta, D'_\theta) \neq 0$, which contradicts the existence of a multiple real root. \square

Before proceeding to the proof of Theorem 1.2, it is instructive to establish the following proposition, which provides a partial result by identifying the intersection of $W(X^w)$ with the real axis. This highlights the underlying structure of the two-matrix model and clarifies why free additive convolution plays a central role in the analysis. For this, we define

$$(3.16) \quad D(x) := D_\theta(x)|_{\theta=0},$$

where D_θ is given by (1.16).

Proposition 3.2. *Let $\alpha \geq 0$ and $0 \leq \tau < 1$. Then the intersection of $W(X^w)$ with the real axis converges almost surely to the real roots of the quartic equation $D(x) = 0$.*

Proof. By the definition of X^w in (1.8), we have

$$(3.17) \quad \text{Re}(X^w) = (1 + \tau)PP^* - (1 - \tau)QQ^*.$$

Note that both $(1 + \tau)PP^*$ and $-(1 - \tau)QQ^*$ are scaled Wishart matrices.

Let μ and ν denote the limiting eigenvalue distributions of $(1 + \tau)PP^*$ and $-(1 - \tau)QQ^*$, respectively. Each of these is a suitably rescaled Marchenko–Pastur distribution. Using the explicit form of the R -transform of the Marchenko–Pastur law (see e.g. [45, Chapter 12]), together with the scaling relation

$$(3.18) \quad R_{cm}(z) = cR_m(cz),$$

it follows that

$$(3.19) \quad R_\mu(z) = \frac{(1 + \alpha)(1 + \tau)}{2 - (1 + \tau)z}, \quad R_\nu(z) = -\frac{(1 + \alpha)(1 - \tau)}{2 + (1 - \tau)z}.$$

Let G denote the Cauchy transform of the free additive convolution $\mu \boxplus \nu$. By the additivity of the R -transform (2.13) and the relation between the R -transform and the Cauchy transform (2.12), we obtain

$$(3.20) \quad \frac{(1 + \alpha)(1 + \tau)}{2 - (1 + \tau)G(z)} - \frac{(1 + \alpha)(1 - \tau)}{2 + (1 - \tau)G(z)} + \frac{1}{G(z)} = z.$$

Rearranging (3.20) yields the cubic equation in $G(z)$:

$$(3.21) \quad z(1 - \tau^2)G(z)^3 + \left((2\alpha + 1)(1 - \tau^2) + 4\tau z\right)G(z)^2 + (4\tau\alpha - 4z)G(z) + 4 = 0.$$

By the Stieltjes inversion formula,

$$(3.22) \quad \frac{d(\mu \boxplus \nu)}{dx}(x) = -\lim_{\epsilon \rightarrow 0} \text{Im} G(x + i\epsilon),$$

the endpoints of the support of $\mu \boxplus \nu$ correspond to those real values of x for which the discriminant D of the cubic equation (3.21) vanishes. Indeed, when $D < 0$, the equation has one real root and a pair of complex conjugate roots, whereas for $D \geq 0$ all roots are real.

Recall that the discriminant of the cubic polynomial is given by

$$(3.23) \quad \text{Disc}(ax^3 + bx^2 + cx + d) = b^2c^2 - 4ac^3 - 4b^3d - 27a^2d^2 + 18abcd.$$

Computing the discriminant of (3.21) and dividing the resulting expression by 16, we obtain a quartic polynomial in z , which coincides precisely with $D(z)$ defined in (3.16). Then, by the well-known almost sure convergence of the extremal eigenvalues for sums of independent Wishart matrices (see e.g. [21, 42] and [31, Theorem 2.3]), together with an application of Lemma 2.2 with $\theta = 0$, the proof is complete. \square

We now prove Theorem 1.2 by extending the previous proposition to a general angle θ , making appropriate use of rotational invariance.

Proof of Theorem 1.2. Let $M = N + v$ and fix $\theta \in [0, 2\pi]$. Define $R := \begin{bmatrix} P & Q \end{bmatrix}$, which is an $N \times 2M$ complex random matrix, where P and Q are the rectangular Ginibre matrices used to define (1.4). Next, set

$$(3.24) \quad T(\theta) := \begin{bmatrix} (1+\tau)\cos\theta & -i\sqrt{1-\tau^2}\sin\theta \\ i\sqrt{1-\tau^2}\sin\theta & -(1-\tau)\cos\theta \end{bmatrix}, \quad S(\theta) := T(\theta) \otimes I_M.$$

A direct computation shows that the eigenvalues of $T(\theta)$ are

$$(3.25) \quad \lambda_{\pm}(\theta) := \tau \cos\theta \pm \sqrt{1 - \tau^2 \sin^2\theta}.$$

Consequently, $S(\theta)$ has the same two eigenvalues, each with multiplicity M .

Note that by (1.4) and (1.8), we have

$$\begin{aligned} RS(\theta)R^* &= \begin{bmatrix} P & Q \end{bmatrix} \begin{bmatrix} (1+\tau)\cos(\theta)I_M & -i\sqrt{1-\tau^2}\sin(\theta)I_M \\ i\sqrt{1-\tau^2}\sin(\theta)I_M & -(1-\tau)\cos(\theta)I_M \end{bmatrix} \begin{bmatrix} P^* \\ Q^* \end{bmatrix} \\ &= \frac{1}{2} \begin{bmatrix} P & Q \end{bmatrix} \begin{bmatrix} \sqrt{1+\tau}I_M & \sqrt{1+\tau}I_M \\ \sqrt{1-\tau}I_M & -\sqrt{1-\tau}I_M \end{bmatrix} \begin{bmatrix} 0 & e^{i\theta}I_M \\ e^{-i\theta}I_M & 0 \end{bmatrix} \begin{bmatrix} \sqrt{1+\tau}I_M & \sqrt{1-\tau}I_M \\ \sqrt{1+\tau}I_M & -\sqrt{1-\tau}I_M \end{bmatrix} \begin{bmatrix} P^* \\ Q^* \end{bmatrix} \\ &= \frac{1}{2} \begin{bmatrix} \sqrt{1+\tau}P + \sqrt{1-\tau}Q & \sqrt{1+\tau}P - \sqrt{1-\tau}Q \end{bmatrix} \begin{bmatrix} 0 & e^{i\theta}I_M \\ e^{-i\theta}I_M & 0 \end{bmatrix} \begin{bmatrix} \sqrt{1+\tau}P^* + \sqrt{1-\tau}Q^* \\ \sqrt{1+\tau}P^* - \sqrt{1-\tau}Q^* \end{bmatrix} \\ &= \frac{1}{2} \left(e^{i\theta} X_1 X_2^* + e^{-i\theta} X_2 X_1^* \right) = \text{Re}(e^{i\theta} X^w). \end{aligned}$$

Since $S(\theta)$ is Hermitian, it admits the spectral decomposition

$$(3.26) \quad S(\theta) = U(\theta) \begin{bmatrix} \lambda_+(\theta)I_M & 0 \\ 0 & \lambda_-(\theta)I_M \end{bmatrix} U(\theta)^*,$$

where $U(\theta)$ is a deterministic $2M \times 2M$ unitary matrix. Consequently,

$$(3.27) \quad \text{Re}(e^{i\theta} X^w) = \tilde{R} \begin{bmatrix} \lambda_+(\theta)I_M & 0 \\ 0 & \lambda_-(\theta)I_M \end{bmatrix} \tilde{R}^*,$$

where $\tilde{R} := RU(\theta)$. Viewing R as consisting of N independent rows of i.i.d. complex Gaussian vectors, the unitary invariance of the Gaussian distribution implies that \tilde{R} has the same distribution as R . Combining the above, we obtain

$$(3.28) \quad \text{Re}(e^{i\theta} X^w) \stackrel{d}{=} R \begin{bmatrix} \lambda_+(\theta)I_M & 0 \\ 0 & \lambda_-(\theta)I_M \end{bmatrix} R^* = \lambda_+(\theta)PP^* + \lambda_-(\theta)QQ^*.$$

The remainder of the argument parallels that of Proposition 3.2. Define μ_θ and ν_θ to be the limiting spectral distributions of $\lambda_+(\theta)PP^*$ and $\lambda_-(\theta)QQ^*$, respectively. Using the R -transform of the Marchenko–Pastur law together with the scaling relation (3.18), we obtain

$$(3.29) \quad R_{\mu_\theta}(z) = \frac{(1+\alpha)\lambda_+(\theta)}{2 - \lambda_+(\theta)z}, \quad R_{\nu_\theta}(z) = \frac{(1+\alpha)\lambda_-(\theta)}{2 - \lambda_-(\theta)z}.$$

Let $G(z)$ denote the Cauchy transform of the free additive convolution $\mu_\theta \boxplus \nu_\theta$. Applying (2.13) and (2.12), we obtain

$$(3.30) \quad z(1 - \tau^2)G(z)^3 + \left((2\alpha + 1)(1 - \tau^2) + 4\tau z \cos(\theta) \right) G(z)^2 + (4\tau\alpha \cos(\theta) - 4z)G(z) + 4 = 0.$$

Notice that for $\theta = 0$, this reduces to (3.21).

Computing the discriminant of the above cubic polynomial with respect to $G(z)$ using (3.23), and dividing the resulting expression by 16, we obtain—after lengthy but straightforward computations—the quartic equation $D_\theta(x) = 0$, where D_θ is defined in (1.16). Then again, by the almost sure convergence of the extremal eigenvalues for sums of independent Wishart matrices, it follows that the largest real root $\lambda(\theta)$ of D_θ coincides with the almost sure limit of $\lambda_{\max}(\theta, N)$. The theorem then follows from Lemma 2.2. \square

4. PROOF OF THEOREM 1.3

In this section, we prove Theorem 1.3. The proof proceeds in two steps. First, in Lemma 4.1, we show that for $n \geq 2$, the numerical range of the product model \mathbf{X}_n^e defined in (1.26) converges, in the large- N limit, to a disc whose radius is independent of the non-Hermiticity parameter. We then determine the explicit form of the radius R_n , which yields the value given in (1.28).

Lemma 4.1. *For $n \geq 2$, let \mathbf{X}_n^e be defined as in (1.26). Then*

$$(4.1) \quad \lim_{N \rightarrow \infty} d_H(W(\mathbf{X}_n^e), \mathbb{D}(R_n)) = 0,$$

almost surely, where R_n is a constant depending only on n .

Proof. Note that by (1.2), the elliptic Ginibre matrix can be decomposed as

$$(4.2) \quad X^e = \sqrt{\frac{1+\tau}{2}} S + i \sqrt{\frac{1-\tau}{2}} T,$$

where S and T are independent GUE matrices. For given semicircular elements $s_1, \dots, s_n, t_1, \dots, t_n$, we define

$$(4.3) \quad u_k := \sqrt{\frac{1+\tau}{2}} s_k + i \sqrt{\frac{1-\tau}{2}} t_k, \quad x_n^e := \operatorname{Re} \left(e^{i\theta} \prod_{k=1}^n u_k \right).$$

For $N \times N$ i.i.d. GUE matrices X_1, X_2, \dots, X_n and free semicircular elements s_1, s_2, \dots, s_n , it was shown in [34] that

$$(4.4) \quad \lim_{N \rightarrow \infty} \|p(X_1, X_2, \dots, X_n)\| = \|p(s_1, s_2, \dots, s_n)\|$$

almost surely, where p is an arbitrary $*$ -polynomial in n variables. By (4.2), (4.3) and (4.4), we have

$$(4.5) \quad \lim_{N \rightarrow \infty} \|\operatorname{Re}(e^{i\theta} \mathbf{X}_n^e)\| = \|x_n^e\|.$$

By (2.3), it suffices to show that $\|x_n^e\|$ is independent of θ and τ . For a free random variable a , it is convenient to adopt the notation

$$a^{\epsilon(\cdot)} = \begin{cases} a, & \text{if } \epsilon(\cdot) = \cdot, \\ a^*, & \text{if } \epsilon(\cdot) = *. \end{cases}$$

Let ϕ denote the tracial state on the underlying non-commutative probability space. Using the definition (4.3) of x_n^e and expanding the m -th power, we obtain

$$(4.6) \quad \phi((x_n^e)^m) = \phi \left(\left(\frac{e^{i\theta} \prod_{k=1}^n u_k + e^{-i\theta} \prod_{k=n}^1 u_k^*}{2} \right)^m \right) = \frac{1}{2^m} \sum_{\epsilon: [m] \rightarrow \{\cdot, *\}} (e^{i\theta})^{\Delta(\epsilon)} \phi(u^{\epsilon(1)} \dots u^{\epsilon(m)}),$$

where

$$\Delta(\epsilon) := |\{k : \epsilon(k) = \cdot\}| - |\{k : \epsilon(k) = *\}|.$$

Here the function $\epsilon : [m] \rightarrow \{\cdot, *\}$ records the choice of terms in the expansion of the product: for each $j \in [m]$, the value $\epsilon(j) = \cdot$ corresponds to selecting the factor $e^{i\theta} \prod_{k=1}^n u_k$, while $\epsilon(j) = *$ corresponds to selecting $e^{-i\theta} \prod_{k=n}^1 u_k^*$. We note that here $\prod_{k=n}^1 u_k^* = u_n^* u_{n-1}^* \dots u_1^*$, and the notation $\prod_{k=n}^1$ is used to emphasise the order of the products.

To evaluate the expectation on the right-hand side of (4.6), we use the moment–cumulant formula of free probability. More precisely, if $NC(k)$ denotes the set of non-crossing partitions of $\{1, \dots, k\}$ and κ_j denotes the j -th free cumulant with respect to ϕ , then for any a_1, \dots, a_k we have

$$\phi(a_1 \cdots a_k) = \sum_{\pi \in NC(k)} \prod_{V \in \pi} \kappa_{|V|}(a_{i_1}, \dots, a_{i_{|V|}}),$$

where for a block $V = \{i_1, \dots, i_{|V|}\}$ we write $\kappa_{|V|}(a_{i_1}, \dots, a_{i_{|V|}})$ for the corresponding free cumulant. Applying this identity to (4.6), we have

$$\phi((x_n^e)^m) = \frac{1}{2^m} \sum_{\epsilon: [m] \rightarrow \{., *\}} (e^{i\theta})^{\Delta(\epsilon)} \sum_{\pi \in NC(mn)} \prod_{\substack{V \in \pi \\ V = \{k_1, \dots, k_j\}}} \kappa_j(u_{k_1}^{\epsilon(i_1)}, \dots, u_{k_j}^{\epsilon(i_j)}).$$

Note that the block $V = \{k_1, \dots, k_j\}$ refers to positions in the word of length mn obtained by expanding

$$(4.7) \quad \prod_{l=1}^m \left(\prod_{k=1}^n u_k \right)^{\epsilon(l)}.$$

More precisely, k_1, \dots, k_j indicate the locations in this word where the entries $u_{k_1}^{\epsilon(i_1)}, \dots, u_{k_j}^{\epsilon(i_j)}$ appear. In particular, each position corresponds to one of the generators u_1, \dots, u_n or their adjoints, and therefore the collection of generator indices occurring in the entire word forms the multiset

$$\{1, \dots, 1, 2, \dots, 2, \dots, n, \dots, n\},$$

where each element $1, \dots, n$ appears exactly m times.

Since the variables u_k are centered and semicircular cumulants vanish for orders different from two, we have $\kappa_j(u_{k_1}^{\epsilon(i_1)}, \dots, u_{k_j}^{\epsilon(i_j)}) = 0$ for $j \neq 2$. Consequently, only pairings contribute to the moment expansion, and therefore

$$(4.8) \quad \phi((x_n^e)^m) = \frac{1}{2^m} \sum_{\epsilon: [m] \rightarrow \{., *\}} (e^{i\theta})^{\Delta(\epsilon)} \sum_{\pi \in NC_2^\epsilon(mn)} \prod_{\substack{V \in \pi \\ V = \{p, q\}}} \kappa_2(u_p^{\epsilon(i)}, u_q^{\epsilon(j)}).$$

Here $NC_2^\epsilon(mn)$ denotes the set of non-crossing pairings of the word of length mn obtained from the expansion of (4.7). As before, we slightly abuse notation when writing p and q : for a block $V = \{p, q\}$ they represent the positions in this length- mn word, whereas in u_p and u_q they indicate the indices of the free generators appearing at those positions.

Since $\kappa_2(u_p^{\epsilon(i)}, u_q^{\epsilon(j)}) = 0$ whenever $p \neq q$, only those non-crossing pairings in $NC_2^\epsilon(mn)$ contribute in which $u_p^{\epsilon(i)}$ and $u_q^{\epsilon(j)}$ are paired if and only if $p = q$. Therefore, each generator u_k can only be paired with another occurrence of the same generator. Since the subscript $k = 1, \dots, n$ appears exactly m times in the length- mn word, this is possible only when m is even.

Suppose that for some k , the elements $u_k^{\epsilon(i)}$ and $u_k^{\epsilon(j)}$ are paired while $\epsilon(i) = \epsilon(j)$. Without loss of generality, assume that $\epsilon(i) = \cdot$. Consider the word of length mn appearing in the expansion of $(x_n^e)^m$. Here the u_k in the first block $(u_1 \cdots u_k \cdots u_n)$ is paired with the u_k in the second block $(u_1 \cdots u_k \cdots u_n)$. Between these two blocks, the word consists of a concatenation of blocks of the form *dot blocks* $(u_1 \cdots u_n)$ or *star blocks* $(u_n^* \cdots u_1^*)$. Let a denote the total number of such blocks occurring between the two blocks containing the paired entries; see Figure 5 for an illustration.

Now consider the subsequence of the elements $u_p^{\epsilon(s)}$ lying between the two paired occurrences of u_k . These elements must themselves form a non-crossing pairing such that $u_p^{\epsilon(s)}$ and $u_q^{\epsilon(t)}$ are paired only if $p = q$. In this subsequence the generator u_k appears exactly a times, hence a must be even. On the other hand, for any $p \neq k$, the generator u_p appears exactly $a + 1$ times, which must also be even for such a pairing to exist. This is impossible, yielding a contradiction (here we use $n \geq 2$).

Therefore the only non-crossing pairings $\pi \in NC_2^\epsilon(mn)$ that contribute are those for which

$$u_p^{\epsilon(s)} \text{ and } u_q^{\epsilon(t)} \text{ are paired} \quad \text{if and only if} \quad p = q \text{ and } \{\epsilon(s), \epsilon(t)\} = \{., *\}.$$

We call such a pairing a *good pairing with respect to ϵ* .

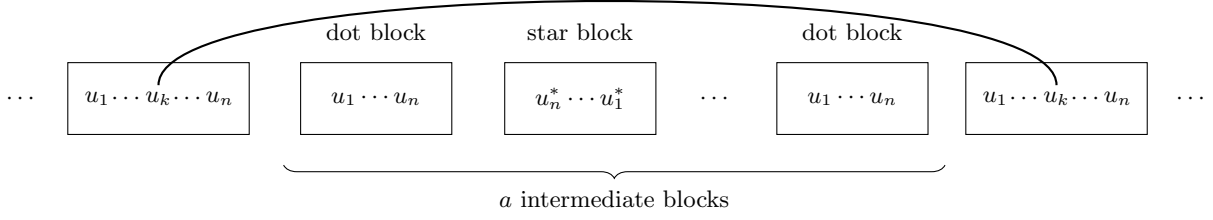


FIGURE 5. Pairing of two occurrences of u_k . The segment between them consists of a intermediate blocks, each being either a dot block ($u_1 \cdots u_n$) or a star block ($u_n^* \cdots u_1^*$).

On the other hand, note that

$$(4.9) \quad \kappa_2(u_k, u_k^*) = \kappa_2\left(\sqrt{\frac{1+\tau}{2}}s_k + i\sqrt{\frac{1-\tau}{2}}t_k, \sqrt{\frac{1+\tau}{2}}s_k - i\sqrt{\frac{1-\tau}{2}}t_k\right) = \frac{1+\tau}{2} + \frac{1-\tau}{2} = 1.$$

Indeed, this is the position where the τ -dependence disappears.

For a good pairing with respect to ϵ to exist, the number of *dot blocks* must equal the number of *star blocks*; equivalently, $\Delta(\epsilon) = 0$. Applying this condition together with (4.9) to (4.8), we obtain

$$(4.10) \quad \phi((x_n^e)^m) = \frac{1}{2^m} \sum_{\substack{\epsilon: [m] \rightarrow \{., *\} \\ \Delta(\epsilon) = 0}} \sum_{\pi \in NC_2^{\epsilon, *}(mn)} 1 = \frac{1}{2^m} \sum_{\pi \in NC_2^*(mn)} 1 = \frac{1}{2^m} |NC_2^*(mn)|.$$

Here $NC_2^{\epsilon, *}(mn)$ denotes the set of good pairings contained in $NC_2^{\epsilon}(mn)$, while

$$(4.11) \quad NC_2^*(mn) := \bigcup_{\substack{\epsilon: [m] \rightarrow \{., *\} \\ \Delta(\epsilon) = 0}} NC_2^{\epsilon, *}(mn)$$

denotes the union of the sets of good pairings over all functions $\epsilon: [m] \rightarrow \{., *\}$ satisfying $\Delta(\epsilon) = 0$.

By (4.10), the moment $\phi((x_n^e)^m)$ is independent of both θ and τ . Consequently, $\|\operatorname{Re}(e^{i\theta} \mathbf{X}_n^e)\|$ is also independent of θ and τ . This completes the proof. \square

By Lemma 4.1, it suffices to treat the case $\tau = \theta = 0$. For circular elements c_1, c_2, \dots, c_n , define

$$(4.12) \quad x_n := \operatorname{Re}\left(\prod_{k=1}^n c_k\right).$$

Then, as before, by [34, Theorem A] (see also [31, Theorem 2.2]) we have

$$(4.13) \quad \lim_{N \rightarrow \infty} \|\operatorname{Re}(\mathbf{X}_n)\| = \|x_n\|,$$

and (4.10) gives

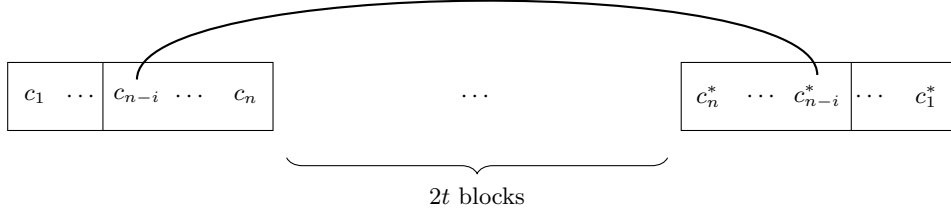
$$(4.14) \quad \phi(x_n^m) = \frac{1}{2^m} |NC_2^*(mn)|.$$

Note that in (4.11), $|NC_2^*(mn)| = 0$ unless m is even, since the numbers of dot blocks and star blocks must agree. Accordingly, we write $m = 2t$ and define

$$(4.15) \quad A_0(t) := |NC_2^*(2nt)|,$$

with the convention that $A_0(0) = 1$. Furthermore, for $1 \leq i \leq n-1$, we define $A_i(t)$ to be the number of good pairings of the subsequence between c_{n-i+1} and c_{n-i+1}^* under the condition that the adjacent entries c_{n-i} and c_{n-i}^* are paired; see Figure 6 for an illustration.

As illustrated in Figure 6, the entries c_{n-i} and c_{n-i}^* are paired, and there are $2t$ blocks between the blocks containing these paired elements. Since the number of dot blocks must coincide with the number of star blocks, the total number of such blocks must be even, which we denote by $2t$. Consequently, there are $2nt$ free random variables between these two blocks, and hence a total of $2nt + 2i$ free random variables involved in the pairing.


 FIGURE 6. The configuration corresponding to $A_i(t)$.

In the case $t = 0$, there is only a single good pairing, and therefore

$$(4.16) \quad A_1(0) = A_2(0) = \cdots = A_{n-1}(0) = 1.$$

Using a simple combinatorial argument, we derive recursive formulas for $A_i(t)$.

Lemma 4.2. *We have*

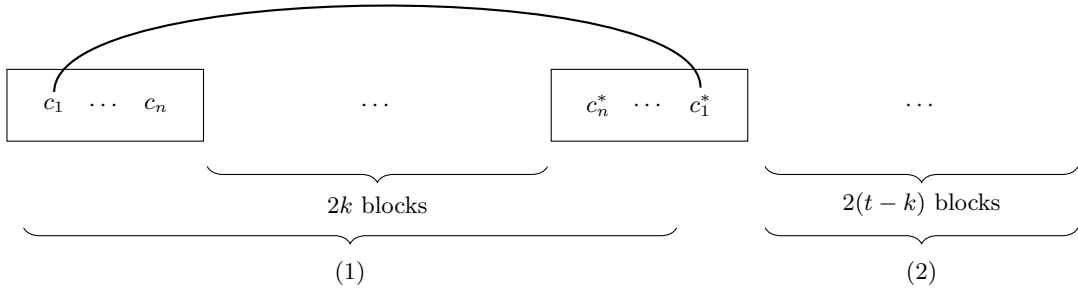
$$(4.17) \quad A_0(t+1) = 2 \sum_{k=0}^t A_{n-1}(k) A_0(t-k)$$

and for $i = 1, \dots, n-1$,

$$(4.18) \quad A_i(t+1) = A_{i-1}(t+1) + \sum_{k=0}^t A_{i-1}(k) \sum_{l=0}^{t-k} A_{n-i-1}(l) A_i(t-k-l).$$

Proof. We first derive the recursive formula for $A_0(t+1)$. The first block may be either a dot block or a star block. By symmetry, it suffices to consider the case where the first block is a dot block; we will multiply the final count by 2 to account for the two possibilities.

Let the first random variable c_1 in the first block be paired with c_1^* in the $(2k+2)$ -th block for some $k = 0, 1, \dots, t$. Note that c_1 cannot be paired with a c_1^* in a $(2k+1)$ -st block, since in that case there would be $2k-1$ blocks between the two paired entries, and hence the numbers of dot and star blocks between them could not be equal. Thus we consider the configuration illustrated in Figure 7.


 FIGURE 7. Configuration contributing to the recursion for $A_0(t+1)$.

The segment (1) contains $2k$ blocks (together with the paired entries c_1 and c_1^* adjacent to them.) Hence the number of good pairings in this region is $A_{n-1}(k)$. On the other hand, the segment (2) contains $2(t-k)$ blocks, which contributes $A_0(t-k)$ admissible pairings.

Combining these contributions and summing over all possible $k = 0, 1, \dots, t$, we obtain (4.17), where the factor 2 accounts for the two possible choices of the first block (dot or star).

Next, we derive a recursive formula for $A_i(t+1)$, where $1 \leq i \leq n-1$. Let the first occurrence of c_{n-i} be paired with c_{n-i}^* in the $(2k+2)$ -th block. As before, it cannot be paired with a copy of c_{n-i}^* in a $(2k+1)$ -st

block, since the numbers of dot and star blocks in between would then be unequal. Here k may take any value in $\{0, 1, \dots, t+1\}$. If $k = t+1$, then the number of good pairings is simply $A_{i-1}(t+1)$.

For the remaining cases $k = 0, 1, \dots, t$, we are led to the configuration shown in Figure 8.

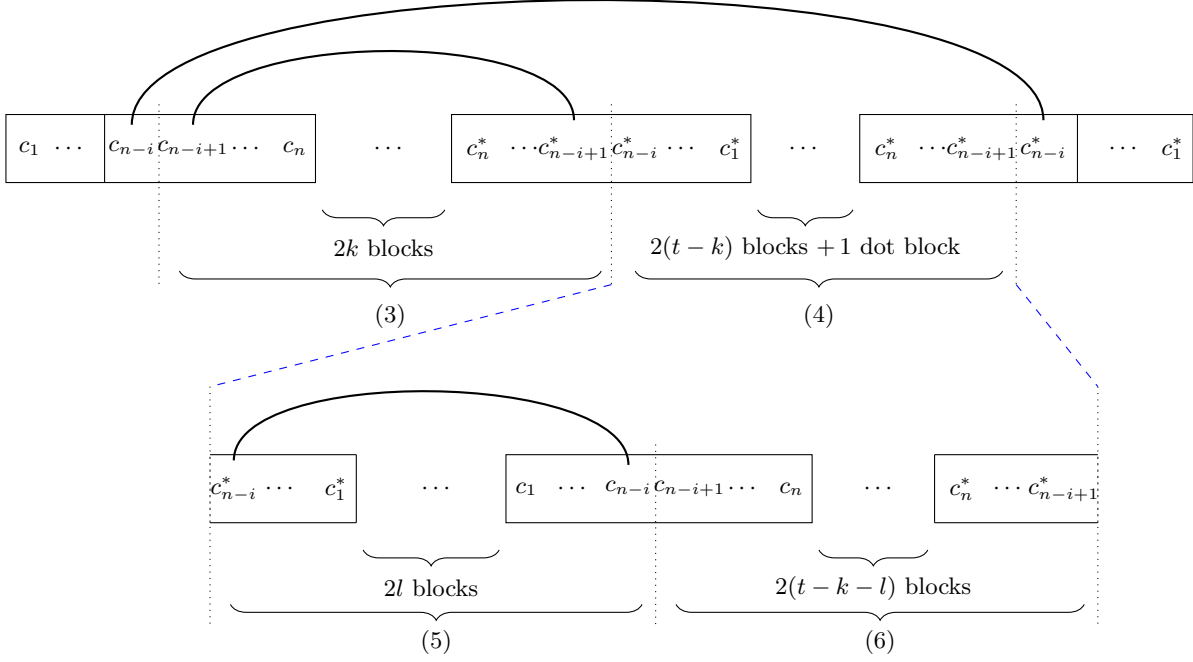


FIGURE 8. Configuration contributing to the recursion for $A_i(t+1)$.

The region labelled (3) contributes $A_{i-1}(k)$. The region labelled (4) is further decomposed according to the position of the first pairing of c_{n-i} , which yields the regions (5) and (6). More precisely, for each $l = 0, 1, \dots, t-k$, the region (5) contributes $A_{n-i-1}(l)$, while the region (6) contributes $A_i(t-k-l)$. Therefore, we obtain (4.18), which completes the proof. \square

We are now ready to prove Theorem 1.3.

Proof of Theorem 1.3. Recall that A_i 's are defined in (4.15) and the text below. For $0 \leq i \leq n-1$, we consider the generating function

$$(4.19) \quad p_i(x) := \sum_{s=0}^{\infty} A_i(s)x^s.$$

Then by (4.17) and (4.18), we have

$$(4.20) \quad p_0(x) - 1 = 2x p_0(x)p_{n-1}(x)$$

and

$$(4.21) \quad p_j(x) - p_{j-1}(x) = x p_{j-1}(x)p_j(x)p_{n-j-1}(x),$$

where $1 \leq j \leq n-1$.

Replacing j by $n-j$ in (4.21), we have

$$(4.22) \quad p_{n-j}(x) - p_{n-j-1}(x) = x p_{n-j-1}(x)p_{n-j}(x)p_{j-1}(x).$$

Dividing (4.21) and (4.22), we obtain

$$(4.23) \quad \frac{p_j(x)}{p_{j-1}(x)} = \frac{p_{n-j}(x)}{p_{n-j-1}(x)}, \quad 1 \leq j \leq n-1.$$

Similarly, for $1 \leq j \leq n-2$, replacing j by $n-j-1$ in (4.21), we obtain

$$(4.24) \quad \frac{p_j(x)}{p_{j-1}(x)} = \frac{p_{n-j-1}(x)}{p_{n-j-2}(x)}, \quad 1 \leq j \leq n-2.$$

Combining the above, we obtain that the ratio $p_j(x)/p_{j-1}(x)$ is constant in j . By denoting

$$(4.25) \quad r(x) := \frac{p_1(x)}{p_0(x)},$$

we have

$$(4.26) \quad p_j(x) = r(x)^j p_0(x), \quad 0 \leq j \leq n-1.$$

We now determine $r(x)$ in terms of $p_0(x)$. Note that by (4.20) and (4.26), we have

$$(4.27) \quad p_0(x) - 1 = 2x r(x)^{n-1} p_0(x)^2.$$

On the other hand, taking $j = 1$ in (4.21), it follows from (4.26) that

$$(4.28) \quad (r(x) - 1)p_0(x) = x r(x)^{n-1} p_0(x)^3.$$

Comparing (4.27) and (4.28), we deduce that

$$(4.29) \quad r(x) = \frac{p_0(x) + 1}{2}.$$

Substituting this into (4.27), we arrive at

$$(4.30) \quad \frac{p_0(x) - 1}{2} = x \left(\frac{p_0(x) + 1}{2} \right)^{n-1} p_0(x)^2.$$

Recall that x_n is given by (4.12). We now consider the moment generating function

$$(4.31) \quad M(z) := 1 + \sum_{m=1}^{\infty} \phi((x_n)^m) z^m.$$

Then by (4.14), (4.15) and (4.19), we have

$$(4.32) \quad M(z) = 1 + \sum_{t=1}^{\infty} \frac{A_0(t)}{2^{2t}} z^{2t} = p_0\left(\frac{z^2}{4}\right).$$

Then the Cauchy transform $G(z)$ of the distribution of the free random variable x_n is given by

$$(4.33) \quad G(z) = \frac{1}{z} M\left(\frac{1}{z}\right) = \frac{1}{z} P_0\left(\frac{1}{4z^2}\right).$$

Then by (4.30), we obtain the algebraic equation

$$(4.34) \quad 2^n(zG(z) - 1) = G(z)^2(zG(z) + 1)^{n-1}.$$

Let

$$(4.35) \quad P(z, w) := w^2(zw + 1)^{n-1} - 2^n(zw - 1).$$

Then $G(z)$ is determined by the equation $P(z, G(z)) = 0$. As before, the endpoints of the support correspond to branch points of this algebraic relation, and hence are obtained by solving

$$(4.36) \quad P(z, w) = 0, \quad \partial_w P(z, w) = 0.$$

From $P(z, w) = 0$ we obtain

$$(4.37) \quad w^2(zw + 1)^{n-1} = 2^n(zw - 1),$$

while $\partial_w P(z, w) = 0$ yields

$$(4.38) \quad (zw + 1)^{n-2}((n+1)zw^2 + 2w) = 2^n z.$$

Solving this system of equations gives

$$(4.39) \quad z = R_n = \sqrt{\frac{\rho_n^2(\rho_n + 1)^{n-1}}{2^n(\rho_n - 1)}}, \quad \rho_n := \frac{1 + \sqrt{1 + 8/n}}{2}.$$

This determines the endpoint of the support, which is the constant R_n given in (1.28), and completes the proof. \square

We end this section by showing that, in the Ginibre matrix case, one may indeed allow repeated factors in the definition of the product model, and that the conclusion of Theorem 1.3 remains valid.

Proposition 4.3. *Let $n \geq 1$ and X_1, X_2, \dots, X_n be $N \times N$ i.i.d. Ginibre matrices. For all $I : [n] \rightarrow [n]$, i.e., $i_1, \dots, i_n \in \{1, \dots, n\}$, denote $\mathbf{X}_I := X_{i_1} X_{i_2} \cdots X_{i_n}$. Then,*

$$(4.40) \quad \lim_{N \rightarrow \infty} d_H(W(\mathbf{X}_I), \mathbb{D}(R_n)) = 0.$$

almost surely, where R_n is given by (1.28).

Proof. Let c_1, c_2, \dots, c_n be circular elements. For an index set $I = (i_1, \dots, i_n)$, define

$$c_I := c_{i_1} c_{i_2} \cdots c_{i_n}, \quad x_I := \operatorname{Re}(c_I).$$

Then, as in the proof of Lemma 4.1, we have

$$(4.41) \quad \lim_{N \rightarrow \infty} \|\operatorname{Re}(\mathbf{X}_I)\| = \|x_I\|.$$

Moreover,

$$(4.42) \quad \phi((x_I)^m) = \frac{1}{2^m} \sum_{\epsilon: [m] \rightarrow \{\cdot, *\}} (e^{i\theta})^{\Delta(\epsilon)} \sum_{\pi \in NC_2^{\epsilon}(mn)} \prod_{\substack{V \in \pi \\ V = \{i_p, i_q\}}} \kappa_2(c_{i_p}^{\epsilon(i)}, c_{i_q}^{\epsilon(j)}).$$

Recall that circular elements satisfy

$$\kappa_2(c_{i_p}^{\epsilon(i)}, c_{i_q}^{\epsilon(j)}) \neq 0 \quad \text{if and only if} \quad i_p = i_q \text{ and } \{\epsilon(i), \epsilon(j)\} = \{\cdot, *\}.$$

Thus, in any contributing pairing, each circular element must be paired with the adjoint of itself.

Consider a good pairing in which c_{i_p} is paired with $c_{i_q}^*$ ($1 \leq p, q \leq n$). Suppose that between these two elements there are t dot blocks and s star blocks. Then the number of circular elements between c_{i_p} and $c_{i_q}^*$ is $n - p + nt$, while the number of adjoint circular elements between them is $n - q + ns$. Since each circular element must pair with the adjoint of itself, these two numbers must coincide, and hence

$$(4.43) \quad n - p + nt = n - q + ns.$$

This implies that $n \mid (p - q)$. As $1 \leq p, q \leq n$, it follows that $p = q$. We have therefore shown that in any good pairing, if c_{i_p} is paired with $c_{i_q}^*$, then necessarily $p = q$.

Now let $J = (j_1, \dots, j_n)$ be another index set. Consider the bijection $c_{i_k} \leftrightarrow c_{j_k}$ ($k = 1, \dots, n$). In this correspondence we regard the symbols c_{i_p} and c_{i_q} as distinct letters whenever $p \neq q$, even if $i_p = i_q$. Under this identification, every good pairing of length mn arising from the expansion of c_I and c_I^* corresponds bijectively to a good pairing arising from the expansion of c_J and c_J^* , and vice versa. Consequently, in the Ginibre case the numerical range does not depend on the index set. \square

APPENDIX A. GEOMETRY OF NUMERICAL RANGE OF NON-HERMITIAN WISHART MATRIX

In this appendix, we expand upon Remark 5 by discussing that the numerical range of the non-Hermitian Wishart matrix in Theorem 1.2 is not an ellipse, despite its apparent resemblance to one.

Let $\xi_+ > \xi_-$ denote the two real roots of $D(x)$ defined in (3.16), and set

$$(A.1) \quad c = \frac{\xi_+ + \xi_-}{2}, \quad A = \frac{\xi_+ - \xi_-}{2}.$$

Suppose that $\tilde{E}(\alpha, \tau)$ is an ellipse. By identifying its major and minor axes, it must then take the form

$$(A.2) \quad \left\{ (x, y) \in \mathbb{R}^2 : \left(\frac{x - c}{A} \right)^2 + \left(\frac{y}{\sqrt{1 - \tau^2} B} \right)^2 \leq 1 \right\},$$

where B is given by (1.21).

The numerical simulations in Figure 9 confirm that the empirical numerical range of the non-Hermitian Wishart ensemble agrees with the set defined in (1.18), rather than with the elliptical approximation in (A.2).

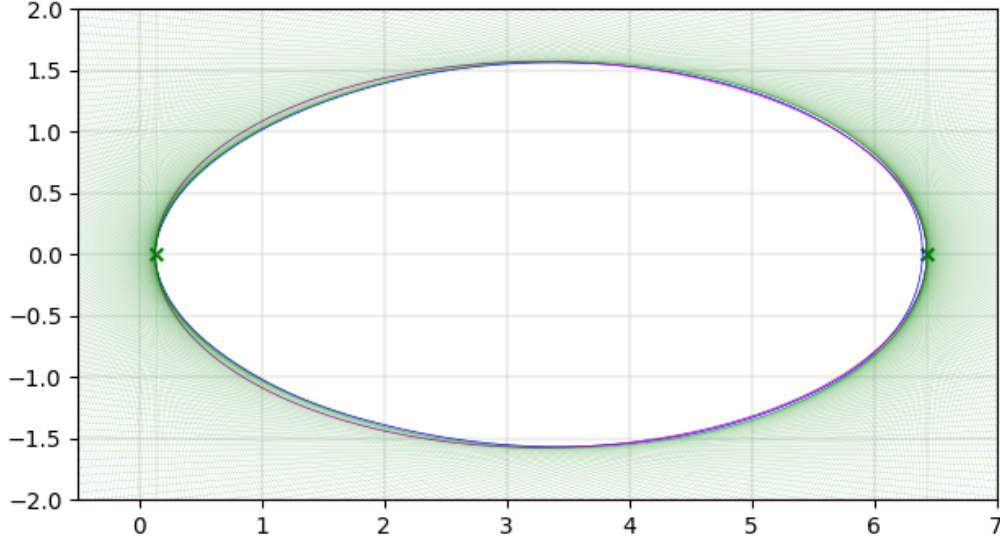


FIGURE 9. The simulated numerical range of the non-Hermitian Wishart matrix (blue solid curve), compared with the theoretical result in Theorem 1.2 (the region bounded by the green envelope), and with the elliptical ansatz (A.2). Here, $\alpha = 2$, $\tau = 0.8$ and $N = 3000$.

In Figure 9, the numerically computed numerical range is shown by the blue curve, while the green lines represent the supporting half-spaces H_θ . The intersection of these half-spaces (the white region bounded by their envelope) corresponds to the theoretical numerical range established in Theorem 1.2. For comparison, the purple curve depicts the ellipse constructed under the heuristic elliptical assumption (A.2). Although the elliptical approximation appears visually close at first glance, a noticeable discrepancy emerges near the boundary close to the leftmost point of the numerical range. In this region, the simulation aligns with our theoretical prediction in Theorem 1.2, rather than with the elliptical ansatz.

One can in fact show analytically that the ansatz (A.2) is false. Indeed, suppose that $\tilde{E}(\alpha, \tau)$ is of the elliptical form (A.2). Then, by (1.18), its support function (cf. (2.10)) is given by

$$c \cos(\theta) \pm \sqrt{A^2 \cos^2(\theta) + (1 - \tau^2)B^2 \sin^2(\theta)}.$$

Consequently, these expressions should coincide with the two real roots of $D_\theta(x) = 0$. Equivalently, $D_\theta(x)$ should admit the factorisation

$$(A.3) \quad \begin{aligned} D_\theta(x) = & \left(x^2 - 2c \cos(\theta)x + (c^2 - A^2) \cos^2(\theta) - (1 - \tau^2)b \sin^2(\theta) \right) \\ & \times \left(16(1 - \tau^2 \sin^2(\theta))x^2 + 32(c - \tau(\alpha + 2))(1 - \tau^2 \sin^2(\theta)) \cos(\theta)x + d_\theta \right), \end{aligned}$$

where $b = B^2$ with B given in (1.21) and

$$(A.4) \quad \begin{aligned} d_\theta = & 16\tau^4 \alpha^2 \cos^4(\theta) + 8\tau^2(1 - \tau^2)(2\alpha^2 - 5\alpha - 6) \cos^2(\theta) + 4(1 - \tau^2)^2(\alpha^2 - 8\alpha - 11) \\ & - 16(c^2 - A^2)(1 - \tau^2 \sin^2(\theta)) \cos^2(\theta) + 16(1 - \tau^2)(1 - \tau^2 \sin^2(\theta))b \sin^2(\theta). \end{aligned}$$

Here, d_θ is determined by matching the coefficients of x^2 .

Comparing the remaining coefficients in (A.3) leads, after lengthy but straightforward computations, to algebraic constraints on the parameters α and τ . Since these identities must hold for all θ , they would force α and τ to satisfy a nontrivial algebraic relation. However, this is impossible, as $\tau \in [0, 1]$ and $\alpha \geq 0$ are free parameters. This contradiction shows that the ansatz (A.2) cannot be valid.

REFERENCES

- [1] G. Akemann and M. Bender, *Interpolation between Airy and Poisson statistics for unitary chiral non-Hermitian random matrix ensembles*, J. Math. Phys. **51** (2010), 103524.
- [2] G. Akemann and Z. Burda, *Universal microscopic correlations for products of independent Ginibre matrices*, J. Phys. A **45** (2012), 465210.
- [3] G. Akemann, S.-S. Byun and N.-G. Kang, *A non-Hermitian generalisation of the Marchenko–Pastur distribution: from the circular law to multi-criticality*, Ann. Henri Poincaré **22** (2021), 1035–1068.
- [4] G. Akemann, S.-S. Byun and K. Noda, *Pfaffian structure of the eigenvector overlap for the symplectic Ginibre ensemble*, Ann. Henri Poincaré (Online), <https://doi.org/10.1007/s00023-025-01575-x>, arXiv:2407.17935.
- [5] G. Akemann, R. Tribe, A. Tsareas and O. Zeitouni, *On the determinantal structure of conditional overlaps for the complex Ginibre ensemble*, Random Matrices Theory Appl. **9** (2020), 2050015.
- [6] J. Alt and T. Krüger, *Local elliptic law*, Bernoulli **28** (2022), no. 2, 886–909.
- [7] Z. Bai and J. W. Silverstein, *Spectral analysis of large dimensional random matrices*, volume 20. Springer, 2010.
- [8] Z. D. Bai, J. W. Silverstein and Y. Q. Yin, *A note on the largest eigenvalue of a large-dimensional sample covariance matrix*, J. Multivariate Anal. **26** (1988), 166–168, 1988.
- [9] Z. D. Bai and Y. Q. Yin, *Limit of the smallest eigenvalue of a large-dimensional sample covariance matrix*, Ann. Probab. **21** (1993), 1275–1294.
- [10] Z. Bao and G. Cipolloni, *Numerical radius of non-Hermitian random matrices*, arXiv:2510.02667.
- [11] Z. Bao, G. Cipolloni, L. Erdős, J. Henheik and O. Kolupaiev, *Decorrelation transition in the Wigner minor process*, Probab. Theory Related Fields (to appear), arXiv:2503.06549.
- [12] Z. Bao, G. Cipolloni, L. Erdős, J. Henheik and O. Kolupaiev, *Law of fractional logarithm for random matrices*, arXiv:2503.18922.
- [13] S. Belinschi, M. A. Nowak, R. Speicher and W. Tarnowski, *Squared eigenvalue condition numbers and eigenvector correlations from the single ring theorem*, J. Phys. A **50** (2017), 105204.
- [14] M. Bender, *Edge scaling limits for a family of non-Hermitian random matrix ensembles*, Probab. Theory Related Fields **147** (2010), 241–271.
- [15] M. Bhattacharjee, A. Bose and A. Dey, *Joint convergence of sample cross-covariance matrices*, ALEA, Lat. Am. J. Probab. Math. Stat. **20** (2023), 395–423.
- [16] P. Bourgade and G. Dubach, *The distribution of overlaps between eigenvectors of Ginibre matrices*, Probab. Theory Related Fields **177** (2020), 397–464.
- [17] Z. Burda, J. Grella, M. A. Nowak, W. Tarnowski and P. Warchol, *Unveiling the significance of eigenvectors in diffusing non-Hermitian matrices by identifying the underlying Burgers dynamics*, Nucl. Phys. B **897** (2015), 421–447.
- [18] S.-S. Byun and P. J. Forrester, *Progress on the study of the Ginibre ensembles*, Springer Singapore, KIAS Springer Series in Mathematics (2025).
- [19] S.-S. Byun and P. J. Forrester, *Electrostatic computations for statistical mechanics and random matrix applications*, arXiv:2510.14334.
- [20] S.-S. Byun and K. Noda, *Scaling limits of complex and symplectic non-Hermitian Wishart ensembles*, J. Approx. Theory **308** (2025), 106148.
- [21] M. Capitaine and C. Donati-Martin, *Strong asymptotic freeness for Wigner and Wishart matrices*, Indiana Univ. Math. J. **56** (2007), 767–803.
- [22] J. T. Chalker and B. Mehlh, *Eigenvector statistics in non-Hermitian random matrix ensembles*, Phys. Rev. Lett. **81** (1998), 3367–3370.
- [23] S. Chang, T. Jiang and Y. Qi, *Eigenvalues of large chiral non-Hermitian random matrices*, J. Math. Phys. **61** (2020), 013508.
- [24] C. Charlier, *Asymptotics of determinants with a rotation-invariant weight and discontinuities along circles*, Adv. Math. **408** (2022), 108600.
- [25] B. Collins, P. Gawron, A. E. Litvak and K. Zyczkowski, *Numerical range for random matrices*, J. Math. Anal. Appl. **418** (2014), 516–533.
- [26] G. Cipolloni, L. Erdős, D. Schröder and Y. Xu, *Directional extremal statistics for Ginibre eigenvalues*, J. Math. Phys. **63** (2022), 103303.
- [27] G. Cipolloni, L. Erdős, D. Schröder and Y. Xu, *On the rightmost eigenvalue of non-Hermitian random matrices*, Ann. Probab. **51** (2023), 2192–2242.
- [28] N. Crawford and R. Rosenthal, *Eigenvector correlations in the complex Ginibre ensemble*, Ann. Appl. Probab. **32** (2022), 2706–2754.
- [29] M. Eiermann, *Fields of values and iterative methods*, Linear Algebra Appl. **180** (1993), 167–197.
- [30] P. J. Forrester, *Log-gases and random matrices*, Princeton University Press, Princeton, NJ, 2010.
- [31] M. Fukuda, T. Hasebe and S. Sato, *Additivity violation of quantum channels via strong convergence to semi-circular and circular elements*, Random Matrices Theory Appl. **11** (2022), 2250012.
- [32] Y. V. Fyodorov, *On statistics of bi-orthogonal eigenvectors in real and complex Ginibre ensembles: combining partial Schur decomposition with supersymmetry*, Comm. Math. Phys. **363** (2018), 579–603.
- [33] Y. V. Fyodorov and W. Tarnowski, *Condition numbers for real eigenvalues in the real elliptic Gaussian ensemble*, Ann. Henri Poincaré **22**, (2021), 309–330.

- [34] U. Haagerup and S. Thorbjørnsen, *A new application of random matrices: $\text{Ext}(C_{red}^*(F_2))$ is not a group*, Ann. of Math. **162** (2005), 711–775.
- [35] K. E. Gustafson and D. K. M. Rao, *Numerical Range: The Field of Values of Linear Operators and Matrices*, Springer-Verlag, New York, 1997.
- [36] F. Hiai and D. Petz, *The semicircle law, free random variables and entropy*, Mathematical Surveys and Monographs, vol. 77, American Mathematical Society, Providence, RI, 2000.
- [37] R. A. Horn and C. R. Johnson, *Topics in Matrix Analysis*, Cambridge University Press, Cambridge, 1994.
- [38] X. Hu and Y. Ma, *Convergence rate of extreme eigenvalue of Ginibre ensembles to Gumbel distribution*, arXiv:2506.04560.
- [39] C. R. Johnson, *Normality and the numerical range*, Linear Algebra Appl. **15** (1976), 89–94.
- [40] E. Kanzieper and N. Singh, *Non-Hermitian Wishart random matrices (I)*, J. Math. Phys. **51** (2010), 103510.
- [41] D.-Z. Liu and Y. Wang, *Universality for products of random matrices I: Ginibre and truncated unitary cases*, Int. Math. Res. Not. IMRN **2016** (2016), 3473–3524.
- [42] J. A. Mingo and R. Speicher, *Free probability and random matrices*, volume 35. Springer, 2017.
- [43] S. Morimoto, M. Katori and T. Shirai, *Generalized eigenspaces and pseudospectra of nonnormal and defective matrix-valued dynamical systems*, arXiv:2411.06472.
- [44] H. H. Nguyen and S. O’Rourke, *The elliptic law*, Int. Math. Res. Not. IMRN **2015** (2015), 7620–7689.
- [45] A. Nica and R. Speicher, *Lectures on the combinatorics of free probability*, volume 335 of London Mathematical Society Lecture Note Series. Cambridge University Press, Cambridge, 2006.
- [46] E. Tadmor, *On the stability of Runge–Kutta methods for arbitrarily large systems of ODEs*, Comm. Pure Appl. Math. **78** (2025), 821–855.
- [47] S. O’Rourke, D. Renfrew, A. Sohnikov and V. Vu, *Products of independent elliptic random matrices*, J. Stat. Phys. **160** (2015), 89–119.
- [48] J. C. Osborn, *Universal results from an alternate random matrix model for QCD with a baryon chemical potential*, Phys. Rev. Lett. **93** (2004), 222001.
- [49] M. A. Stephanov, *Random matrix model of QCD at finite density and the nature of the quenched limit*, Phys. Rev. Lett. **76** (1996), 4472.
- [50] Y. Xu and Q. Zeng, *Large deviations for the extremal eigenvalues of Ginibre ensembles*, arXiv:2512.12711.

DEPARTMENT OF MATHEMATICAL SCIENCES AND RESEARCH INSTITUTE OF MATHEMATICS, SEOUL NATIONAL UNIVERSITY, SEOUL 151-747, REPUBLIC OF KOREA

Email address: sungsoobyun@snu.ac.kr

COLLEGE OF MEDICINE, SEOUL NATIONAL UNIVERSITY, SEOUL 151-747, REPUBLIC OF KOREA

Email address: jyp531@snu.ac.kr